GERMAN - MONGOLIAN INSTITUTE FOR RESOURCES AND TECHNOLOGY

The present work was submitted to

the German-Mongolian Institute for Resources and Technology

Study on Vibration-Based Energy Harvesting from Industrial Machinery Vibration for Low-Power Sensor Devices Use

Bachelor's Thesis

By

TULGA Avarga

Study program: Mechatronics Engineering

Student ID: B2100570

1st Supervisor/Examiner: Prof. Ph.D Odbileg.N

2nd Supervisor/Examiner: Prof. M.Sc Myagmarjav.B

Ulaanbaatar/Nalaikh

2025

GERMAN - MONGOLIAN INSTITUTE FOR RESOURCES AND TECHNOLOGY

The present work was submitted to

the German-Mongolian Institute for Resources and Technology

Study on Vibration-Based Energy Harvesting from Industrial Machinery Vibration for Low-Power Sensor Devices Use

Bachelor's Thesis

By

TULGA Avarga

Study program: Mechatronics Engineering

Student ID: B2100570

1st Supervisor/Examiner: Prof. Ph.D Odbileg.N

2nd Supervisor/Examiner: Prof. M.Sc Myagmarjav.B

Ulaanbaatar/Nalaikh

2025

Statutory Declaration

Avarga TULGA B2100570

I hereby affirm in lieu of an oath that I provided the submitted bachelor thesis

Study on Vibration-Based Energy Harvesting from Industrial Machinery Vibration for Low-Power Sensor Devices Use

I did not use any sources other than those stated. In case that the work is additionally submitted on a data medium, I declare that the written and the electronic form are completely identical. The work was not submitted in the same or similar form to any examination authority.

28.05.2025 Tulga. A

Place, Date Signature

Acknowledgment

First of all, I would like to express my deepest gratitude to my university, German Mongolian Institute for Resources and Technology for their support, providing me with various opportunities to learn and become a Mechatronics engineer.

I would like to express my sincere gratitude to my first supervisor, Prof. Ph.D Odbileg.N, for his invaluable guidance and insightful comments throughout my thesis. His ability to connect theoretical concepts with real-life engineering problems helped me develop a deeper understanding of practical applications. His shared experiences and mentorship greatly contributed to my perspective on solving real-world challenges. I am also thankful to him for providing essential measurement tools that played a crucial role in the experimental phase of this work.

I am also grateful for my second supervisor, Prof. M.Sc Myagmarjav.B, for his continuous support and constructive feedback. His expertise in software development and signal processing formed the backbone of the analytical part of my thesis. I am especially grateful for his thorough explanations, which enhanced my understanding of key technical concepts and methods.

My sincere thanks go to Bold.E, assistant at the Energy and Electrical Engineering laboratory, for his help during the electrical measurement procedures. I also extend my appreciation to Amarsanaa.I, assistant at the Mechanical laboratory, for his assistance in conducting the mechanical measurement sessions.

Lastly, I would like to thank my parents for their relentless financial and emotional support. Their efforts in creating a supportive environment enabled me to concentrate on my research and complete this thesis to the best of my ability.

Abstract

The growing demand for sustainable and maintenance-free power sources in industrial environments has driven the exploration of ambient energy harvesting technologies. This thesis investigates the use of vibration-based energy harvesting from industrial machinery as a power source for low-power sensor devices. By focusing on piezoelectric transduction, the study presents the design, modeling, and testing of a small-scale energy harvester prototype built around Arduino, piezoelectric elements, and passive power electronics.

Field measurements were conducted on vibrating machinery such as motors and pumps operating at 30 Hz and 50 Hz to characterize real-world excitation sources. A cantilever piezoelectric beam made of PZT-5A was designed and analyzed using ANSYS Workbench to determine its natural frequency and harmonic response. The harvester's electrical behavior was simulated using MATLAB/Simulink, and the system's real-time performance was evaluated using a function generator, oscilloscope, and the MPU6050 accelerometer module.

The results showed that the harvested voltage ranged from a few hundred millivolts up to ~1.0 V depending on vibration intensity. The time-domain and frequency-domain analysis revealed a clear correlation between vibration frequency and harvested voltage. The system reliably activated an LED when the voltage exceeded threshold levels, confirming functionality. Simulation results closely matched experimental data, supporting the validity of the proposed model.

This work concludes that piezoelectric vibration energy harvesting is a viable power solution for autonomous industrial sensor applications. While not yet suitable for continuous power delivery, the proposed system can effectively support intermittent sensing tasks, reducing battery dependence and enabling sustainable deployment of low-power monitoring devices.

Table of Contents

List of Tables

List of Figures

List of Abbreviations

1. EM – Electromagnetic
2. WEC – Wave energy converters
3. MMR – Mechanical-motion-rectifier
4. VEH – Vibration energy harvester
5. IoT – Internet of Things

6. FEM – Finite Element Method
7. PZT – Lead, Zirconate, Titanate
8. FFT – Fast Fourier Transform
9. WSN – Wireless Sensor Network

List of Equations

$$\mathrm{mz}^{\cdot\cdot} + \mathrm{cz}^{\cdot} + \mathrm{kz} = -\mathrm{my}^{\cdot\cdot} - F_{em}(\mathrm{t}) \quad (1)$$

$$F_{em}(\mathrm{t}) = \mathrm{NB}\ell\mathrm{i}(\mathrm{t}) \Leftrightarrow \mathrm{e}(\mathrm{t}) = -\mathrm{NB}\ell\mathrm{z}^{\cdot}(\mathrm{t}) \quad (2)$$

$$\delta = \frac{1}{\gamma}\sigma + dE \quad (3)$$

$$D = d\sigma + \varepsilon E \quad (4)$$

$$F = \frac{q^2}{2a_e\varepsilon_0} - k_{sp}z \quad (5)$$

$$q = C(z)V \quad (6)$$

$$C(z) = \frac{a_e\varepsilon_0}{d-z} \quad (7)$$

$$k^2 = \frac{d^2}{s*\varepsilon} = \frac{d^2*Y}{\varepsilon} \quad (8)$$

$$E = \frac{CV^2}{2} \quad (9)$$

$$V_{out} = V_{in} * \frac{R_2}{R_1+R_2} \quad (10)$$

$$V_{out} = \frac{V_{in}}{2} \quad (11)$$

$$I = \frac{V}{R},\ P = V * I \quad (12)$$

$$A(f) = \sum_{n=0}^{N-1} a(n) * e^{-j2\pi fn/N} \quad (13)$$

$$\begin{bmatrix} S \\ D \end{bmatrix} = \begin{bmatrix} s & d \\ d & \varepsilon \end{bmatrix} \begin{bmatrix} T \\ E \end{bmatrix} \quad (14)$$

$$k^2 = \frac{d^2}{S\varepsilon} = \frac{d^2Y}{\varepsilon} \quad (15)$$

1. Introduction

1.1 Motivation

The modern industrial sector increasingly relies on sensor networks for predictive maintenance, condition monitoring, process optimization, and safety assurance. However, powering these vast networks remains a critical challenge. Traditional battery solutions impose considerable maintenance challenges, particularly in inaccessible locations, resulting in elevated labor expenses and environmental issues related to battery disposal. Recent statistics show that billions of batteries are discarded every year, adding to environmental pollution and resource depletion.

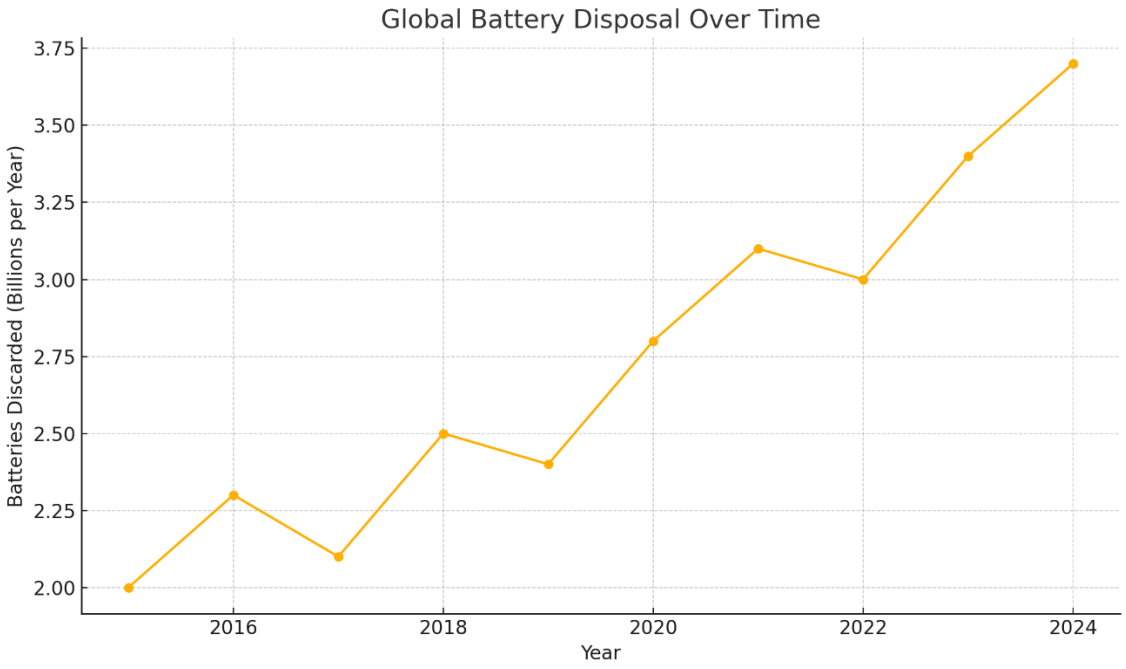

Figure 1. Increase in global battery disposal from 2015 to 2024.

In parallel, vibration is a silent yet powerful energy source in these industries. Machines such as motors, pumps, compressors, and conveyors generate continuous mechanical oscillations during operation, typically at frequencies well-suited for energy harvesting. Though relatively low in energy compared to larger renewable sources like wind or solar, these vibrations are more than sufficient for operating modern ultra-low-power electronics, especially with advancements in microelectronic fabrication and sensor technologies that have drastically reduced power consumption.

This realization became even more evident to me during my internship experiences at Vitafit LLC and the MAK Euro Block Factory. Throughout my time at these facilities, I observed numerous motors and pumps operating continuously, day and night, producing noticeable noise and persistent vibrations. During these observations, the idea stuck with me: the vibrational energy generated by these machines, typically overlooked and wasted, holds potential as a usable energy source. Recognizing this untapped opportunity to contribute to sustainable industrial practices inspired me to select this topic for my bachelor's thesis.

Thus, the motivation for this study arises naturally from the convergence of three trends: the need for autonomous, maintenance-free sensor systems, the abundant presence of exploitable vibration energy in industrial environments, and the maturity of energy harvesting technologies that can efficiently convert mechanical motion into usable electrical power. Successfully tapping into this energy offers a sustainable solution to the problems of battery maintenance, sensor downtime, and waste generation while promoting the implementation of intelligent, self-powered industrial systems.

1.2 Background

Energy harvesting has emerged as a key technology for supporting the long-term operation of wireless sensor networks (WSNs) and Industrial Internet of Things (IoT) systems. Traditional battery-powered sensors face serious limitations, particularly in harsh or remote industrial environments where maintenance access is difficult and costly. As industries strive towards more autonomous and sustainable systems, alternative power sources have become increasingly critical.

Among the various ambient energy sources — such as solar, thermal gradients, and human motion — mechanical vibrations present a promising opportunity in industrial settings. Machines like motors, pumps, and compressors operate continuously, generating vibrations typically in the 30–300 Hz range, with measurable amplitudes and accelerations often exceeding 0.5–1.0 g. These conditions are ideal for vibration-based energy harvesting, which converts mechanical energy into electrical energy (1).

Compared to human motion, which usually produces lower frequencies (<10 Hz) and less predictable vibrations, industrial machinery provides a much more stable and powerful energy source. Studies have shown that typical industrial vibration environments can yield energy densities of 10–100 microwatts per cubic centimeter ($\mu W/cm^3$), sufficient for modern ultra-low-power sensors, many of which operate below 50 microwatts.

Various transduction methods are employed to harvest vibrational energy, each with its advantages:

- Piezoelectric harvesting, which uses materials like PZT (lead zirconate titanate), can efficiently generate relatively high voltages from mechanical strain.
- Electromagnetic harvesting relies on relative motion between a magnet and a coil, producing current according to Faraday's law of induction.
- Electrostatic harvesting uses the changing capacitance between charged plates to generate energy, particularly suited for MEMS-scale devices.

This study will focus on piezoelectric vibration energy harvesting (VEH) due to its high energy density, simplicity, and compatibility with compact, low-maintenance sensor deployments. Combining piezoelectric materials with modern ultra-low-power electronics offers a highly promising pathway for creating fully autonomous industrial sensor systems.

1.3 Research Objectives

The primary objective of this thesis is to explore the practical viability of vibration-based energy harvesting from industrial machinery for powering low-power sensor devices. Specifically, the following goals have been set:

- **Objective 1: Analyze Vibration Characteristics of Industrial Machinery**

Field measurements will be conducted on typical industrial machines such as pumps and motors. Data on vibration frequencies, amplitudes, and spectral characteristics will be collected and analyzed to identify suitable energy harvesting opportunities.

- **Objective 2: Evaluate and Compare Transducer Technologies**

This study presents a theoretical comparison of electromagnetic, piezoelectric, and electrostatic energy harvesting methods based on efficiency, durability, and compatibility with industrial vibrations. Only the piezoelectric method will be experimentally tested, while the others are compared using literature-based data.

- **Objective 3: Design and Develop a Small-Scale Vibration Energy Harvester Prototype**

Based on the findings from Objectives 1 and 2, a small-scale prototype will be developed using Arduino for control and preliminary data acquisition. The prototype will aim to efficiently harvest energy from machine-induced vibrations and store it for sensor operation.

- **Objective 4: Validate the Prototype in Real-world Conditions**

The prototype's performance will be tested under real industrial conditions to evaluate its ability to power low-energy sensor devices consistently. MATLAB/Simulink modeling will be used to simulate system behavior, while ANSYS Workbench will assist in analyzing material properties and mechanical responses.

- **Objective 5: Assess Feasibility for Sustainable Sensor Deployment**

Finally, the feasibility of deploying vibration-based energy harvesters as a sustainable alternative to battery-powered sensors will be assessed, considering factors like energy autonomy, maintenance reduction, economic viability, and environmental benefits.

2 Literature Review

2.1 Recent Research and Trends

Vibration-based energy harvesting, an approach for transforming mechanical vibration into usable electrical power, has gained significant attention from researchers due to its broad applicability. As illustrated in Figure 2, the number of publications exploring vibration-based energy harvesters has shown a clear upward trend in recent years. Figure 3 provides a detailed breakdown of these research contributions according to country. To date, approximately 5,000 scholarly articles have been published on this emerging subject from researchers across more than 10 countries. The following sections present a comprehensive overview of vibration-based energy harvesting, covering key aspects such as energy conversion mechanisms, common sources of vibration, energy harvesting devices coupled with vibration control capabilities, and broadband energy harvesting techniques.

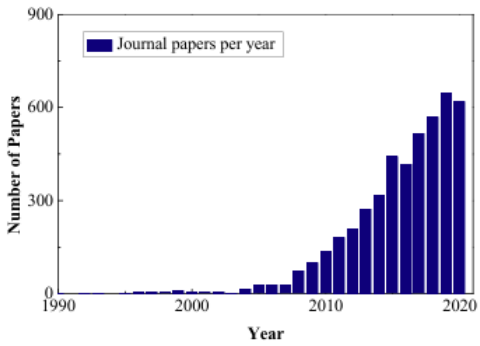

Figure 2. Number of papers published per year in the field of vibration-based energy (1)

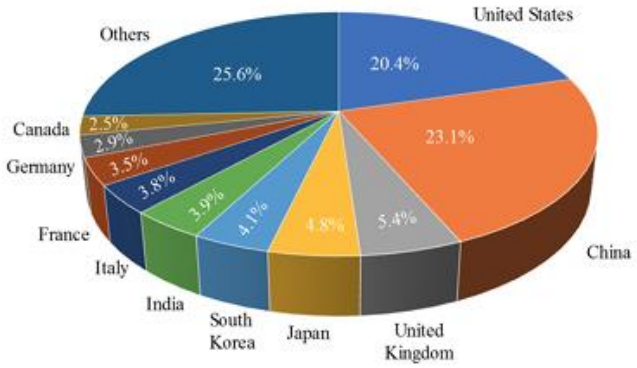

Figure 3. Distribution by country of papers on vibration-based energy harvesting (1)

Numerous extensive evaluations have examined this subject from multiple perspectives. Preliminary research, by Sod04 (2) and Ant07 (3) examined piezoelectric energy harvesting, focusing on design geometry and improvements in efficiency. Bee06 (4) examined vibration-based energy harvesting at the microsystem level, whereas Sta18 (5) presented updates on recent developments. Supplementary analyses by She12 (6), Wei17 (7), and Iqb21 (8) focused on power conditioning techniques, transduction mechanisms, and microsystem applications.

This section briefly introduces fundamental concepts related to vibration-based energy harvesting, including transduction mechanisms, vibration sources, energy harvesting methods, and their applications in low-power sensor devices.

2.2 Vibration as an Energy Source

In virtually every environment around us, mechanical vibrations are an abundant—and until recently, largely untapped—reservoir of energy. Everyday sources span from human activities (walking, running, even arterial pulses) and vehicle motions (engine idling, road-induced chassis shake) to industrial machinery (motors, pumps, compressors), HVAC systems, and even ocean or river waves. Each source is characterized by a dominant frequency band (from sub-Hz in civil structures up to several hundred Hz in rotating equipment) and an associated acceleration amplitude (typically 0.01–3 g in industrial settings and 0.2–2 g in human motion). By matching a vibration-harvesting device to the specific Hz and g-level of its target source, we can recover electrical power directly from the otherwise wasted mechanical oscillations. Table 1 summarizes representative vibration sources, operating frequencies, and typical

acceleration levels—information critical when selecting or tuning an energy harvester for a given application.

Vibration Source	Typical Frequency (Hz)	Acceleration (g)
Industrial induction motors	25-60	0.5-1.5
Centrifugal pumps	20-200	0.6-2.0
Air compressors	100-300	0.8-2.5
Machine tools (lathe, milling)	90-150	0.5-1.2
Washing machines	~80	0.02
Vibratory compactors	~136	0.8
HVAC fans (industrial)	50-120 (1x and harmonics)	0.2-0.6
Bridges and large civil structures	0.1-3	0.01-0.2
Automotive engines (idle to cruise)	30-150	0.3-1.0
Rotating shafts (e.g., pumps, turbines)	30-300	0.5-2.0
Human walking	1-3	0.2-0.8
Human running	2-5	0.5-2.0

Table 1. Representative vibration sources, their dominant frequency ranges, and typical acceleration levels.

2.2.1 Railway Tracks

Passing trains induce 0.6–1.8 Hz vibrations in railway tracks with 3–7 mm peak deflection, making the tracks a viable power source. Early field trials by Nel08 (9) showed that simple electromagnetic (EM) and piezoelectric harvesters could yield 4 mW and 0.05 mW from track motion. Subsequent EM prototypes, including ones with hydraulic transmission or mechanical motion rectifiers (MMRs), boosted efficiency to over 50% and delivered watts of power. For example, Wan13 (10) used an MMR to drive a generator lighting two 50 W bulbs at 1 Hz. In parallel, sleeper-mounted piezoelectric designs (patch, stack, and drum types) have demonstrated tens to hundreds of milliwatts under realistic loading and have even powered microcontrollers in field tests. Overall, EM harvesters tend to reach watt-level outputs, while piezoelectric versions produce hundreds of milliwatts more often.

2.2.2 Ocean Waves

Ocean waves offer a highly predictable, high-density power source—on the order of 2–3 kW/m²—yet commercial wave-energy converters (WECs) remain at an early stage of development. Among WEC types, point absorbers (devices smaller than a

wavelength) are particularly attractive because they can be arrayed to scale up power capture. Most of these devices work in heavy mode; for instance, an electromagnetic (EM) point absorber with a mechanical-motion-rectifier (MMR) generated about 21 W during sea tests, and prototypes like the Smart Power Buoy, which is rated at 300 W, are currently being tested for commercial use (11). Although heave is most commonly exploited, surge and pitch motions actually contain twice the extractable energy, and devices such as SEAREV and PeWEC have begun to tap these modes. Piezoelectric buoys have also been designed in various ways—from film-array models (Burn 1987) to lever-amplified cantilever systems—forecasting energy outputs from hundreds of milliwatts to tens of watts in larger installations that are about a meter in size.

2.2.3 Industrial Machinery

Mechanical oscillations are one of the most abundant and underutilized energy reservoirs in industrial settings. Rotating machinery, such as induction motors and centrifugal pumps, routinely exhibit measurable vibration signatures during normal operation that can be harvested. Typical full-load induction motors generate dominant fundamental vibration components at 25–60 Hz (corresponding to rotational speeds of 3,000–1,500 rpm), with root-mean-square (RMS) acceleration levels often in the 0.5–1 g range. Likewise, centrifugal pumps vibrate primarily in the 20–200 Hz band, driven by hydraulic and mechanical forces, with accelerations up to 2 g under heavy duty. (12)

Vibration Source	Fundamental Frequency (Hz)	RMS Acceleration (g)
Industrial induction motors	25-60	0.5-1.0
Centrifugal pumps	20-200	0.6-2.0
Air compressors	100-300	0.8-2.5

Table 2. Typical vibration characteristics of industrial motors and pumps

Because such machinery often runs continuously at near-steady speeds, its vibration is both persistent and predictable, a major advantage over diurnal or weather-dependent sources like solar or wind.

2.3 Energy Harvesting Mechanisms

A standard arrangement of vibration-based energy harvesters consists of a linear or nonlinear oscillator, wherein the damping energy can be partially transformed into

electrical energy via suitable energy transducers, including piezoelectric, electromagnetic, and electrostatic transducers. Figure 4.

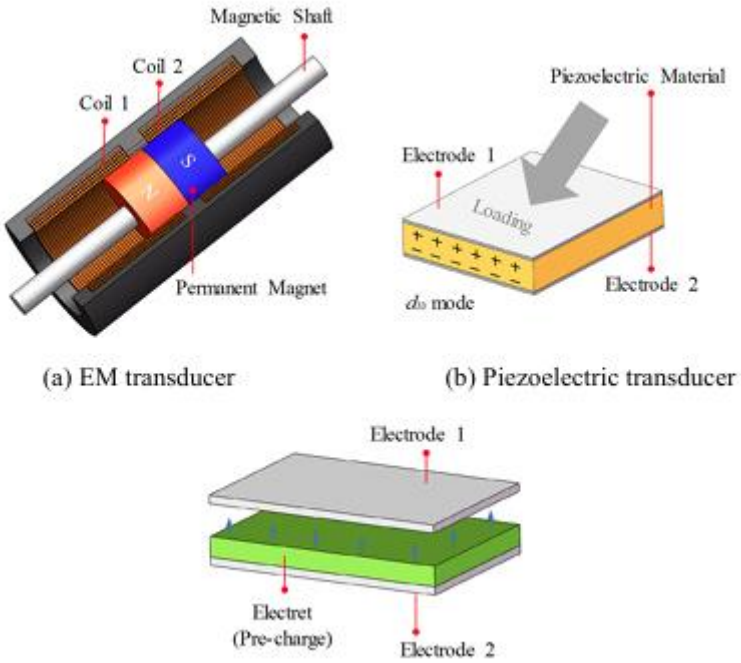

Figure 4. Three main types of transducers

2.3.1 EM Transducer

Electromagnetic harvesters exploit Faraday's law: as a magnet and coil move relative to one another, an induced voltage drives current. The simplest form is a single-degree-of-freedom inertial oscillator mounted within a housing, which has been used at scales from backpacks, where a suspended-load EM generator produced several watts during normal walking, to large civil structures such as high-rise buildings, bridges, railways, and ocean-wave point absorbers. Because EM generators excel at low frequencies and high-power levels and inherently provide a controllable damping force, they are well suited to vibration control in addition to power generation. However, miniature EM harvesters tend to produce relatively low voltages, and their efficiency and output grow with transducer size, limiting their use in weight- or space-constrained applications.

Here are the key governing equations for a simple single-degree-of-freedom electromagnetic (EM) vibration harvester:

1. Mechanical equation of motion

   For a mass m on a spring–damper subjected to base excitation y(t):

$$mz^{\cdot\cdot} + cz^{\cdot} + kz = -my^{\cdot\cdot} - F_{em}(t) \quad (1)$$

where:

- $z(t) = x(t) - y(t)$ is the relative displacement of the mass
- c is the mechanical (parasitic) damping,
- k is the spring stiffness,
- $F_{em}(t)$ is the electromagnetic reaction (Lorentz) force

2. Lorentz force & induced voltage

When a coil of N turns, each of length ℓ, moves with velocity $z^{\cdot}$ in a (nominally) uniform flux density B.

$$F_{em}(t) = NB\ell i(t) \Leftrightarrow e(t) = -NB\ell z^{\cdot}(t) \quad (2)$$

2.3.2 Piezoelectric Transducer

Piezoelectric materials, a class of ferroelectrics, develop internal dipoles under mechanical stress, generating an electric charge, the direct piezoelectric effect. The converse effect, where applied voltage induces mechanical stress, enables actuation. These behaviors are described by the constitutive relations:

$$\delta = \frac{1}{\gamma}\sigma + dE \quad (3)$$

$$D = d\sigma + \varepsilon E \quad (4)$$

where δ is strain, σ stress, Y Young's modulus, d the piezoelectric coefficient, E the electric field, and D is the electric displacement. The coupling term in Equations (3) and (4) clearly links the mechanical and electrical domains, illustrating how piezoelectric materials transduce mechanical forces or vibrations into electrical energy.

The dominant design for VEH examined in literature is the cantilever geometry. This is due to the fact that a specific applied force results in the cantilever beam design yielding the maximum average strain. In the development of vibration-based energy harvesters employing piezoelectric materials, the resonance frequency of the device corresponds to the frequency at which optimal electrical output is attained. This frequency depends on the device's setup, dimensions, and loading circumstances. For numerous ambient vibration sources, vibration frequencies typically remain below 200 Hz. Recent studies have concentrated on diminishing the resonance frequencies of these energy-collecting devices to enhance their performance in ambient vibration conditions. In previous years, Glynne-Jones et al. created a trapezoidal lead zirconate titanate (PZT) cantilever with a steel substrate, which generated 3 μW of electricity while

functioning at a frequency of 80 Hz. Roundy et al. created a PZT bimorph cantilever measuring 1 cm^3, functioning at roughly 80 μW with a frequency of 100 Hz. Subsequently, they developed a multi-degree-of-freedom system employing several springs and masses. This gadget might generate a wider frequency range for better performance**.** (13)

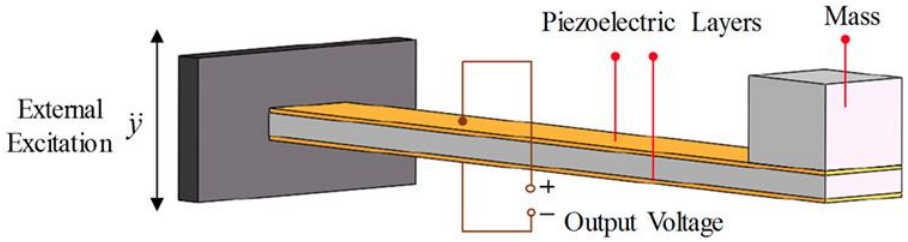

Figure 5. Beam-type piezoelectric energy harvester

2.3.3 Electrostatic Transducer

The fundamental basis of electrostatic vibration-based energy harvesting is Coulomb's Law. Electrostatic energy harvesters operate via variations in the capacitance of two parallel plate capacitors, which are usually electrically isolated by air, vacuum, or an insulating material. The attraction forces between these two oppositely charged components vary with the distance between them. Consequently, by altering the capacitance of vibration-sensitive conductors, mechanical energy from vibrations can be transformed into electrical energy. A comprehensive elucidation of this methodology is provided by SMe01, (14) which proposes a hybrid technique utilizing parasitic capacitance to enhance power production.

Assuming constant charge operation and ignoring any parasitic capacitance, the coupled constitutive equations are:

$$F = \frac{q^2}{2a_e\varepsilon_0} - k_{sp}z \tag{5}$$

$$q = C(z)V \tag{6}$$

$$C(z) = \frac{a_e\varepsilon_0}{d-z} \tag{7}$$

Where F, q is the charge, V is the voltage across the capacitor, a_e is the electrode area, ε_0 is the permittivity constant, and C(z) is the capacitance of the structure.

2.3.4 Comparison

Transducer type	Electromagnetic	Piezoelectric	Electrostatic
Harvesting principle	EM induction	Piezoelectric effect and electrostatic induction	Electrostatic induction
Impedance type	Resistive	Capacitive	Capacitive
Practical maximum energy storage density (mJ/cm^3)	24.8	35.4	4
Pros	• High output current, power, and efficiency • Easy to scale up • High durability • Low output impedance • Tuning is possible at low, medium, and high vibration levels	• Easy to scale down to nanoscale • Simple structure on a small scale • High coupling coefficient • High output voltage	• Lightweight • Very high output voltage • Easy for frequency tuning • Competitive in its compact size • Compatibility with microelectromechanical technology
Cons	• Heavy magnet required • Low voltage for small-scale devices	• Low output current and efficiency • Pulsed output • High matched impedance • Brittle • Low strain limit	• Pre-charge required • Low output current • High matched impedance • High resonant frequency required

Table 3. Comparison of different energy transducers in vibration-based EH

Note: This information and data are from the reports by Wang (2017) (15), Park et al. (2019) (16), and Siddique et al (2015) (17).

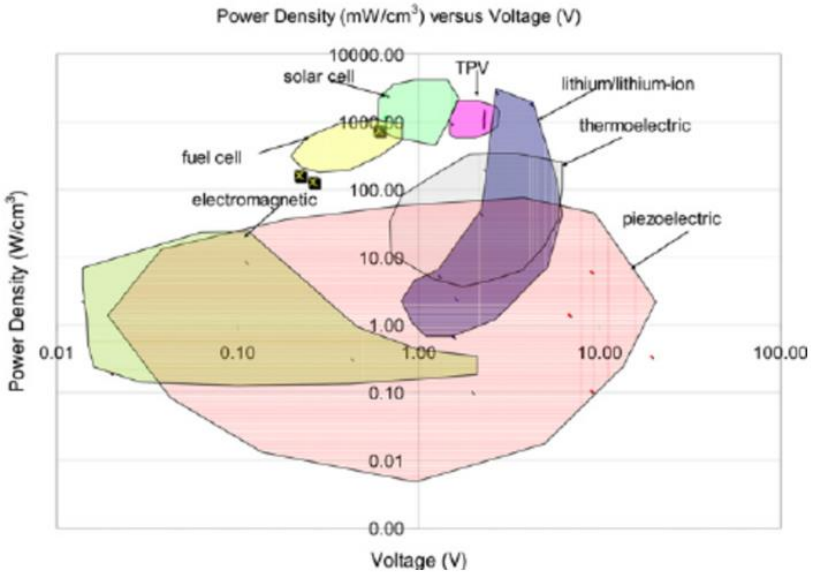

Figure 6. Plot of power density versus voltage for common regenerative and lithium/lithium-ion power supply strategies. (From Cook-Chennault et al (2008) (18)

I selected piezoelectric materials to model because, as Figure 6 and Table 6 show, they offer a simple, small-scale structure while delivering both high power density and high output voltage.

2.4 Application for Low-Power Sensor Devices

Vibration-based energy harvesting (VEH) is a promising solution for powering low-power wireless sensor devices in industrial environments. These sensors—used for condition monitoring, temperature, or vibration measurement—typically require between 10 µW and 1 mW, especially when duty-cycled to operate intermittently.

Wireless sensor nodes typically consist of sensing elements, microcontrollers for data processing, and wireless communication modules. These components exhibit ultra-low power demands, often ranging from 10 µW to several milliwatts depending on the sensor type and operational duty cycle. For instance, commercial acceleration sensors such as the ADXL330 from Analog Devices consume approximately 324 µW, while temperature sensors like the STLM20 from STMicroelectronics require only 11.52 µW under standard conditions (19).

In a pivotal experimental study by Waterbury and Wright, a compact electromagnetic VEH prototype (2.5 cm^3) was demonstrated to effectively power sensor nodes in industrial environments. From a 15–30 kW pump motor, 0.2 to 1.5 mW was harvested, while face milling operations yielded up to 1.9 mW from machine tool vibrations. These power levels are sufficient to meet or exceed the duty-cycled energy requirements (typically 1% duty) of commercial wireless sensors, such as those used for condition monitoring and predictive maintenance.

In terms of energy storage and regulation, VEH systems are often coupled with supercapacitors or rechargeable micro batteries to manage fluctuations in harvested energy and ensure reliable power delivery. These storage elements bridge the gap between the intermittent nature of vibrations and the continuous power demand of electronic circuitry. Hybrid energy management systems incorporating voltage regulators and power management ICs can further optimize energy flow from the harvester to the load, enabling uninterrupted operation of sensor nodes during periods of low vibration input (20).

3 Methodology

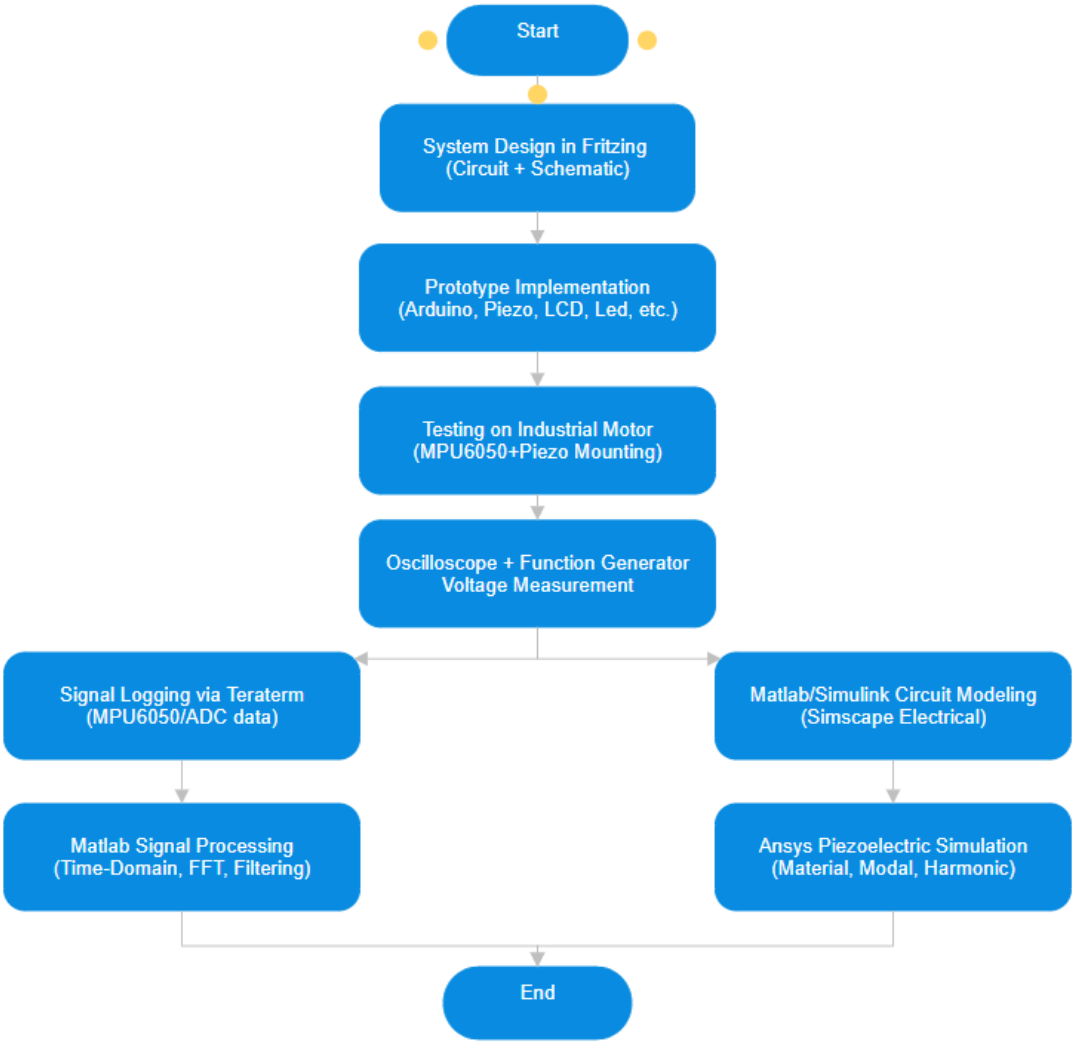

Figure 7. Methodology flowchart outlining system design, testing, and analysis

3.1 System Design and Prototype Implementation

The core objective of the prototype was to demonstrate the feasibility of harvesting electrical energy from mechanical vibrations using piezoelectric transducers and to visualize the harvested voltage in real time through an I2C LCD display and LED indicator system. Additionally, an MPU6050 accelerometer module was integrated to measure the actual vibration levels applied to the piezoelectric elements, providing insight into the correlation between mechanical input and electrical output. The system was designed and assembled using commonly available electronic components and microcontroller

modules, with the design phase carried out using Fritzing software to generate both the breadboard layout and schematic diagram (Figure 8 and Figure 9).

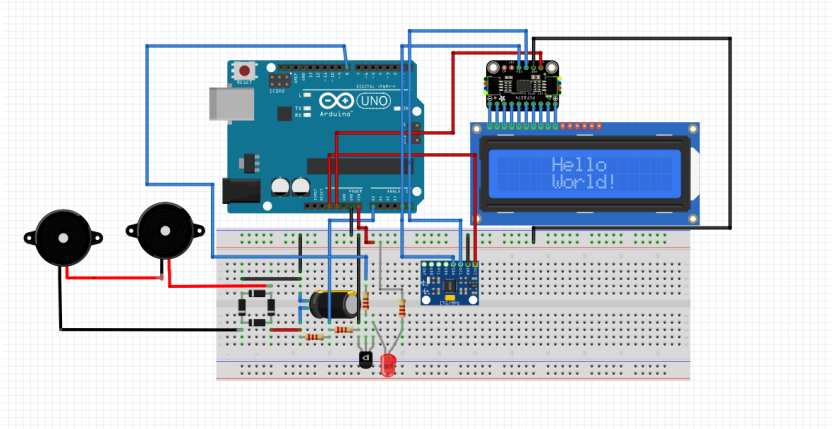

Figure 8. Circuit diagram

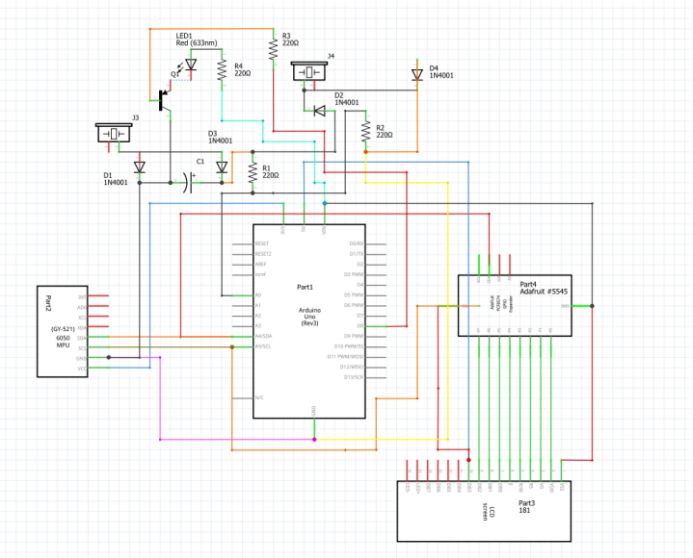

Figure 9. Schematic diagram of the circuit

The prototype consists of the following main components:

Microcontroller: Arduino Uno R3 serves as the central processing unit for voltage reading and I2C LCD communication.

Piezoelectric transducers: Two identical piezo elements were connected in series to increase the cumulative voltage output under mechanical stress or vibration.

From the constitutive relation, we can find the piezoelectric coupling coefficient using:

$$k^2 = \frac{d^2}{s*\varepsilon} = \frac{d^2*Y}{\varepsilon} \quad (8)$$

Assuming:

$d = 300 * 10^{-12} C/N$

$Y = 6.3 * 10^{10} N/m^2$

$\varepsilon = 1500 * \varepsilon_0 = 1500 * 8.85 * 10^{-12} F/m$

$$k^2 = \frac{(300e^{-12})^2 * 6.3e^{10}}{(1500 * 8.85e^{-12})} \approx 0.428$$

This shows a relatively high coupling efficiency for PZT-5A material.

Bridge rectifier: A W005M full-wave bridge rectifier was used to convert the AC output from the piezo elements into a unidirectional DC signal.

Capacitor: A 100 µF electrolytic capacitor was connected across the output of the rectifier to smoothen the rectified voltage and store energy momentarily.

To find energy stored in the capacitor:

$$E = \frac{CV^2}{2} \quad (9)$$

Where:

$$C = 100\mu F = 100 * 10^{-6} F$$

$$V = 3.2$$

$$E = 0.5 * 100e^{-6} * 3.2^2 = 512\mu J$$

Resistors and transistors: A BC547 NPN transistor and 10 kΩ resistors were used to control the switching logic for lighting an LED when the harvested voltage exceeds a certain threshold. Resistors were also used as a voltage divider to ensure that the harvested voltage remains below 5V to protect the Arduino from potential damage.

To safely measure the capacitor voltage with the Arduino's analog input (maximum 5V), a voltage divider circuit was included using two equal-value resistors (10 kΩ each). The divided voltage sent to the analog pin is given by:

$$V_{out} = V_{in} * \frac{R_2}{R_1 + R_2} \quad (10)$$

With $R_1 = R_2 = 10kOhm$

$$V_{out} = \frac{V_{in}}{2} \quad (11)$$

If the capacitor voltage (V_in) reaches 3.2 V, then:

$V_{out} = \frac{3.2}{2} = 1.6V$ (Safe for Arduino analog pin)

Display module: An I2C LCD (Adafruit #5545) was interfaced with the Arduino to display real-time voltage readings retrieved from the analog input pin.

Indicator: A red LED was used as a visual indicator to show when the harvested voltage reached a usable level.

To find power delivered to the load:

$$I = \frac{V}{R} = \frac{3.2}{220} = 14.5mA,\ P = V * I = 3.2V * 14.5e^{-3} = 46mW \quad (12)$$

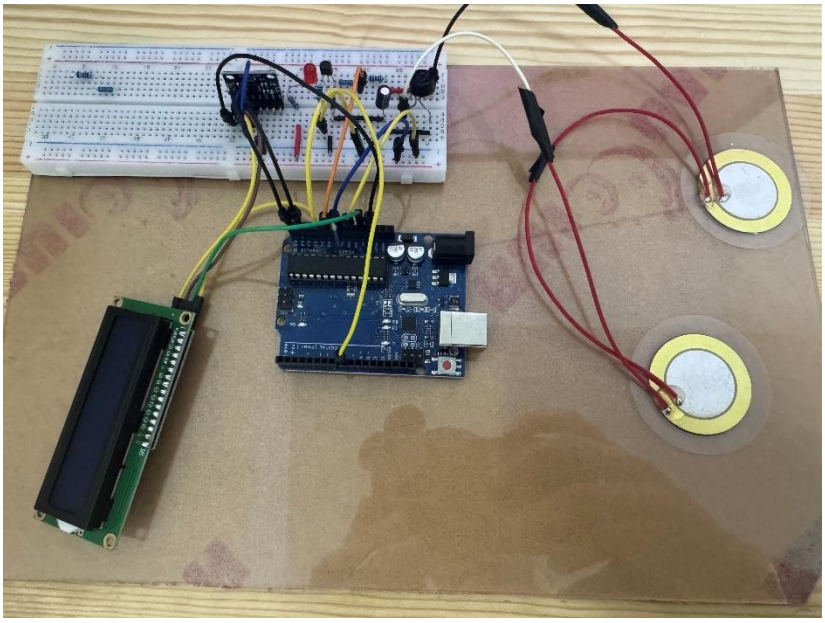

Figure 10. Circuit setup

Figure 11 demonstrates the real-world circuit setup, where the user applies finger pressure on the piezo elements to simulate vibrational stimuli. The LED lights up only when the harvested voltage reaches a level sufficient to forward-bias the transistor.

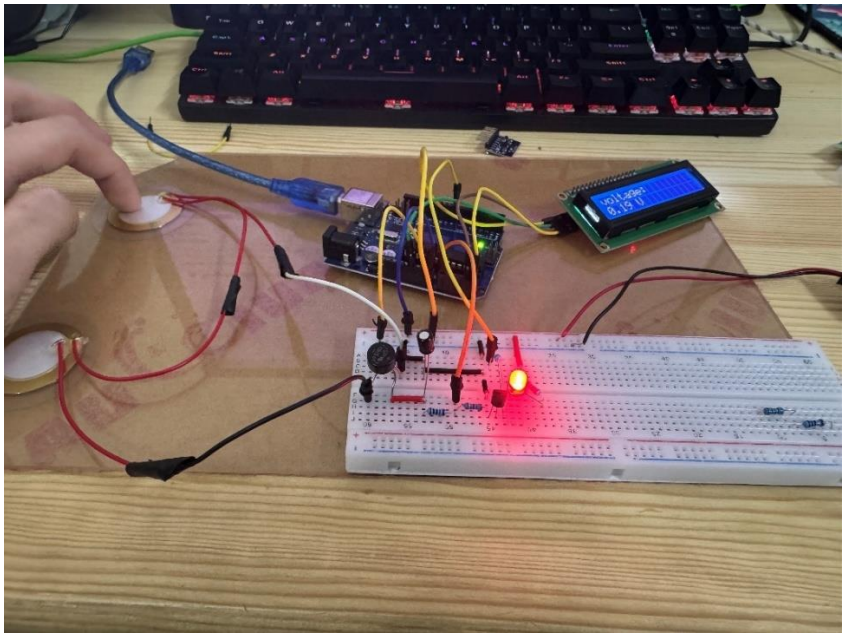

Figure 11. Circuit setup with finger vibration

The entire circuit was designed in Fritzing, both as a breadboard layout and a schematic diagram, to ensure clean wiring and logical component placement. These diagrams (Figure 8 and Figure 9) served as a reliable reference during physical implementation and documentation. Each connection was verified using a digital multimeter (Figure 12) and voltage measurements across the capacitor showed values ranging from a few millivolts up to ~1.0V depending on the intensity and frequency of the applied vibration.

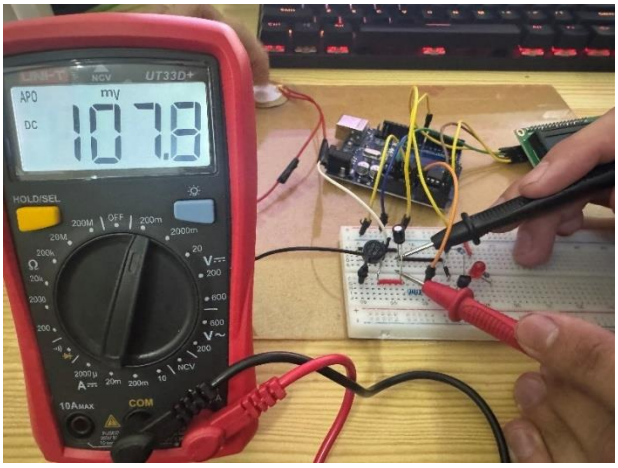

Figure 12. Multimeter measurement across the capacitor.

3.2 Laboratory Measurements and Data Acquisition

This phase focused on capturing voltage output from the piezoelectric energy harvester system and correlating it with mechanical vibrations using measurement instruments and controlled signal inputs. The goal was to validate circuit behavior under real-world and simulated vibration conditions.

3.2.1 Testing on Industrial Motor

For real-world testing, the piezoelectric discs were mounted on the casing of an operational industrial motor to harvest vibrations produced during rotation. The motor speed was varied to approximate frequencies of 30 Hz and 50 Hz. A GY-521 MPU6050 6-axis accelerometer module was attached to the same surface to measure vibration intensity across all three axes. The sensor was connected to an Arduino Uno via I2C, and its output was visualized using the Arduino Serial Plotter.

This allowed for synchronized acquisition of both mechanical input (vibration acceleration) and electrical output (harvested voltage) under different RPM conditions.

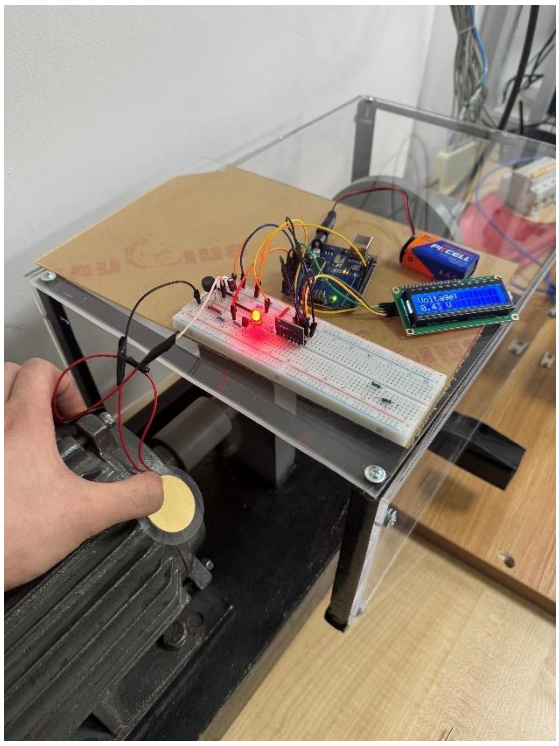

Figure 13. Testing on motor

Figure 14. Measuring vibration characteristics

3.2.2 Oscilloscope and Function Generator-based Voltage Measurement

A Tektronix TDS 2024C digital oscilloscope (200 MHz, 2 GS/s) was used to monitor voltage levels at various stages of the circuit:

- Before the bridge rectifier (pure piezo AC signal)
- After the bridge rectifier (pulsating DC)
- Across the capacitor (smoothed and stored DC)

These measurements were used to understand waveform characteristics, frequency response, and energy conversion behavior. The oscilloscope's time and voltage scaling were adjusted appropriately depending on the expected output range. To replicate consistent vibrations and isolate the piezo's frequency response, a function generator was used to simulate a sine wave signal at specific known frequencies—30 Hz and 50 Hz. This helped in calibrating the system's behavior without relying solely on physical vibration inputs, allowing precise control over amplitude and frequency.

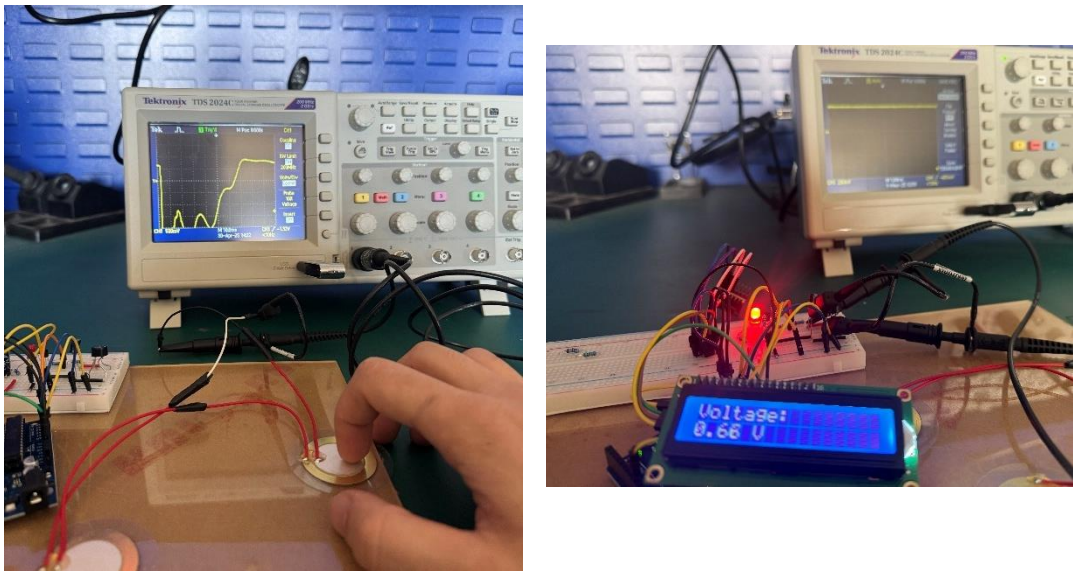

Figure 15. Oscilloscope measurement

3.3 Signal Processing and Frequency Analysis Using Matlab

To investigate the relationship between mechanical vibrations and the voltage generated by the piezoelectric energy harvester, signal acquisition and processing were performed using a combination of Arduino-based sensing and MATLAB analysis. The MPU6050 accelerometer and piezoelectric voltage output were connected in parallel to

an Arduino Uno, enabling the simultaneous acquisition of tri-axial vibration and rectified voltage data. This configuration allowed for direct correlation between the mechanical input and the resulting electrical output of the system.

Raw data, including time, voltage, and acceleration values, were transmitted from the Arduino to a laptop using Tera Term terminal software and saved as .csv files for offline processing. Each dataset corresponded to different motor excitation frequencies (30 Hz and 50 Hz), replicating real operating conditions. Additionally, oscilloscope waveforms of the piezoelectric output were captured in digital format to enable synchronized time-domain and frequency-domain analysis. These combined datasets were processed in Matlab using custom scripts to identify dominant vibration frequencies, apply signal filtering, and interpret the relationship between acceleration and harvested voltage for energy analysis.

The first stage involved time-domain inspection of acceleration signals. The raw data a(t) was plotted to observe vibration trends, identify outliers, and understand signal amplitude over time. To extract frequency information, the Fast Fourier Transform (FFT) was applied:

$$A(f) = \sum_{n=0}^{N-1} a(n) * e^{-j2\pi fn/N} \quad (13)$$

where a(n) is the discrete acceleration signal and N is the total number of samples. The FFT revealed dominant frequency components — typically around the motor's operational frequency.

```
% FFT Analysis
Fs = 1 / mean(diff(time)); % Sampling frequency
L = length(voltage);
Y = fft(voltage);
P2 = abs(Y/L);              % Two-sided spectrum
P1 = P2(1:floor(L/2)+1);    % Single-sided spectrum
P1(2:end-1) = 2*P1(2:end-1);
f = Fs*(0:(L/2))/L;         % Frequency domain

figure;
plot(f, P1);
xlim([0 100]);
title('FFT Analysis');
xlabel('Frequency (Hz)');
ylabel('|P1(f)|');
grid on;
```

Figure 16. FFT Analysis on Matlab

```
% Peak Detection
[peaks, locs] = findpeaks(voltage, 'MinPeakProminence', 0.02);

figure;
plot(time, voltage); hold on;
plot(time(locs), peaks, 'ro');
title('Peak Detection in Voltage Signal');
xlabel('Time (s)');
ylabel('Voltage (V)');
legend('Signal', 'Peaks');
grid on;
```

Figure 17. Peak detection of the frequency

To reduce high-frequency noise, a low-pass Butterworth filter was implemented using Matlab's butter and filter functions. The filter cutoff frequency was selected just above the dominant vibration frequency to retain meaningful components while eliminating artifacts. This cleaned signal was then used to compare acceleration data with the harvested voltage.

The voltage and acceleration were plotted together in a time series and also compared using scatter plots. This allowed for a qualitative assessment of the relationship between mechanical vibration intensity and electrical energy output. For each test frequency, the average harvested voltage was also computed and plotted to observe trends in energy conversion efficiency as a function of vibration frequency.

3.4 Simulation Tools

To gain deeper insight into the behavior of the vibration-based piezoelectric energy harvesting system, numerical modeling and Multiphysics simulations were conducted using MATLAB/Simulink and ANSYS Workbench. These simulations enabled a theoretical validation of circuit-level behavior and mechanical-electrical coupling phenomena in piezoelectric materials, facilitating design optimization prior to hardware implementation.

In MATLAB/Simulink, the full circuit model was constructed using the Simscape Electrical toolbox. The system included a sinusoidal vibration source (representing environmental mechanical excitation), a piezoelectric bender with electrical coupling, a full-wave bridge rectifier, an energy storage capacitor, and a load interface incorporating a switching transistor. A 50 Hz sine wave was applied as the input excitation to match typical industrial motor vibration frequencies observed during testing. The simulation allowed observation of transient current flow, power dissipation across passive elements, and

capacitor charging behavior in response to the input waveform. These parameters were analyzed with respect to time, and their behavior was compared with theoretical expectations based on RC circuit dynamics.

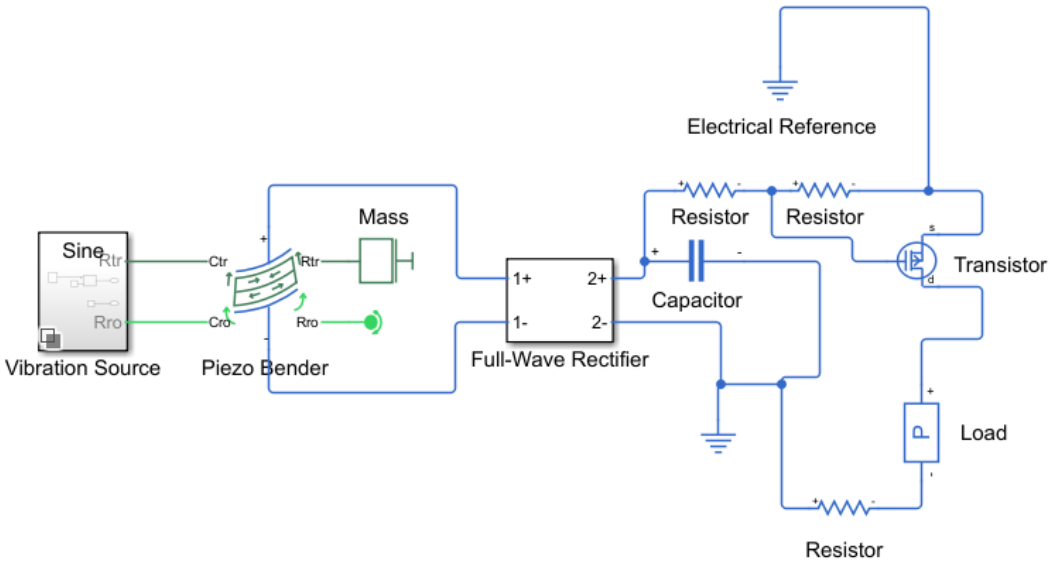

Figure 18. Circuit model on the Matlab/Simulink

The behavior of the piezoelectric component was further studied in ANSYS Workbench using the Finite Element Method (FEM). A cantilever beam structure made of PZT-5A piezoelectric ceramic was modeled with a point mass attached at the free end to amplify vibrational strain. The mechanical boundary conditions replicated a fixed-free cantilever configuration, and a harmonic force was applied to simulate vibration input. The material properties (Figure 20, Figure 21, and Figure 22) of PZT-5A were defined in terms of its density, piezoelectric strain coefficients, and dielectric permittivity. The mechanical response was coupled with the electrical domain using the anisotropic material stiffness matrix and piezoelectric constitutive equations.

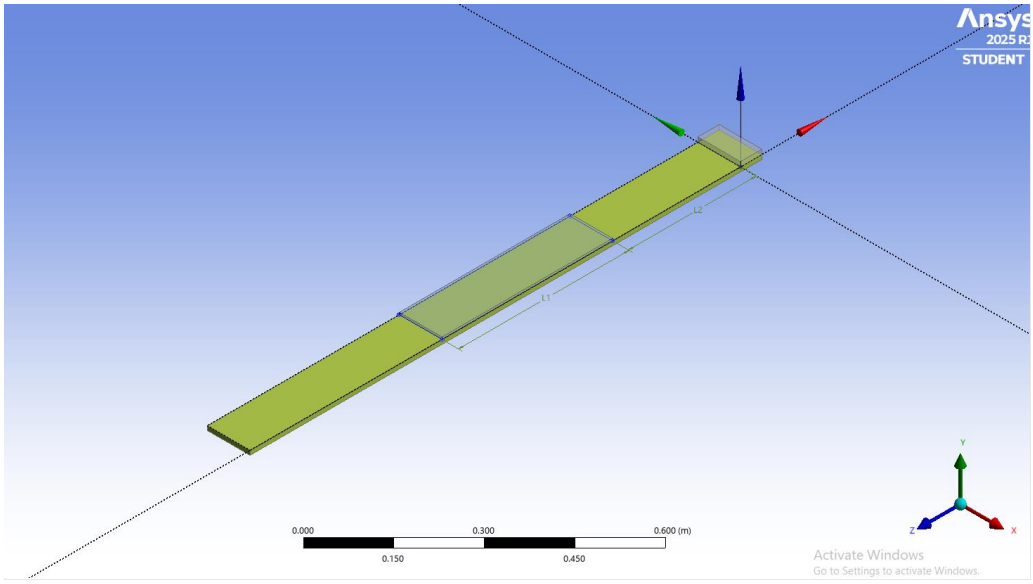

Figure 19. Cantilever PZT-5A model on Ansys

Table of Properties Row 4: Anisotropic Elasticity

	A	B	C	D	E	F
1	D[*,1] (Pa)	D[*,2] (Pa)	D[*,3] (Pa)	D[*,4] (Pa)	D[*,5] (Pa)	D[*,6] (Pa)
2	1.2E+11					
3	7.51E+10	1.15E+11				
4	7.52E+10	7.51E+10	1.2E+11			
5	0	0	0	2.11E+10		
6	0	0	0	0	2.11E+10	
7	0	0	0	0	0	2.26E+10

Figure 20. Stiffness matrix of the PZT-5A

Table of Properties Row 8: Anisotropic Relative Permittivity

	A	B	C
1	εS[*,1]	εS[*,2]	εS[*,3]
2	1.9926E-09		
3	0	5.7838E-10	
4	0	0	1.9926E-09

Figure 21. Strain matrix of the PZT-5A

Table of Properties Row 10: Piezoelectric Matrix

	A	B	C
1	e[*,1] (coulomb m^-2)	e[*,2] (coulomb m^-2)	e[*,3] (coulomb m^-2)
2	0	-5.3512	0
3	0	15.783	0
4	0	-5.3512	0
5	12.295	0	0
6	0	0	12.295
7	0	0	0

Figure 22. Piezo element finite element matrix

The constitutive equations for piezoelectric materials describe the coupling between mechanical and electrical domains and are given in matrix form as:

$$\begin{bmatrix} S \\ D \end{bmatrix} = \begin{bmatrix} s & d \\ d & \varepsilon \end{bmatrix} \begin{bmatrix} T \\ E \end{bmatrix} \tag{14}$$

where S is the strain, D is the electric displacement, s is the mechanical compliance, d is the piezoelectric strain coefficient, ε is the dielectric permittivity, T is the applied mechanical stress, and E is the electric field. These relations form the basis of Multiphysics simulation in ANSYS for predicting electrical output based on mechanical deformation.

The coupling efficiency of a piezoelectric material can be described by the electromechanical coupling coefficient k^2, which quantifies the proportion of mechanical energy converted to electrical energy. It is derived from the constitutive relations and expressed as:

$$k^2 = \frac{d^2}{S\varepsilon} = \frac{d^2 Y}{\varepsilon} \tag{15}$$

where Y is the Young's modulus of the material. This parameter is crucial for selecting piezoelectric materials for energy harvesting applications, as a higher coupling coefficient implies a more efficient conversion process.

Modal analysis in ANSYS was used to extract natural frequencies of the cantilever structure, which are essential for matching the system's resonance with environmental vibration sources. Harmonic response analysis provided the amplitude-frequency characteristics under a range of excitation frequencies. Finally, voltage generation at the piezoelectric surface electrodes was computed, which depends on the localized strain distribution and the material's electromechanical properties.

4 Results and Analysis

This chapter presents and compares the simulation and experimental results obtained from the piezoelectric energy harvesting system. The outcomes are grouped based on the modeling platform (MATLAB/Simulink, ANSYS Workbench) and the empirical measurements obtained through oscilloscope and function generator. A comparative analysis highlights the consistency between the modeled system behavior and physical implementation.

4.1 ANSYS Workbench Modal and Harmonic Analysis

Modal analysis performed in ANSYS Workbench revealed the first three natural frequencies of the PZT-5A cantilever beam with a tip mass: 5.15 Hz, 34.37 Hz, and 50.10 Hz (**Error! Reference source not found.**, Figure 25, and Figure 25). The first mode exhibited maximum deformation at the free end, indicating the primary resonance condition suitable for energy harvesting.

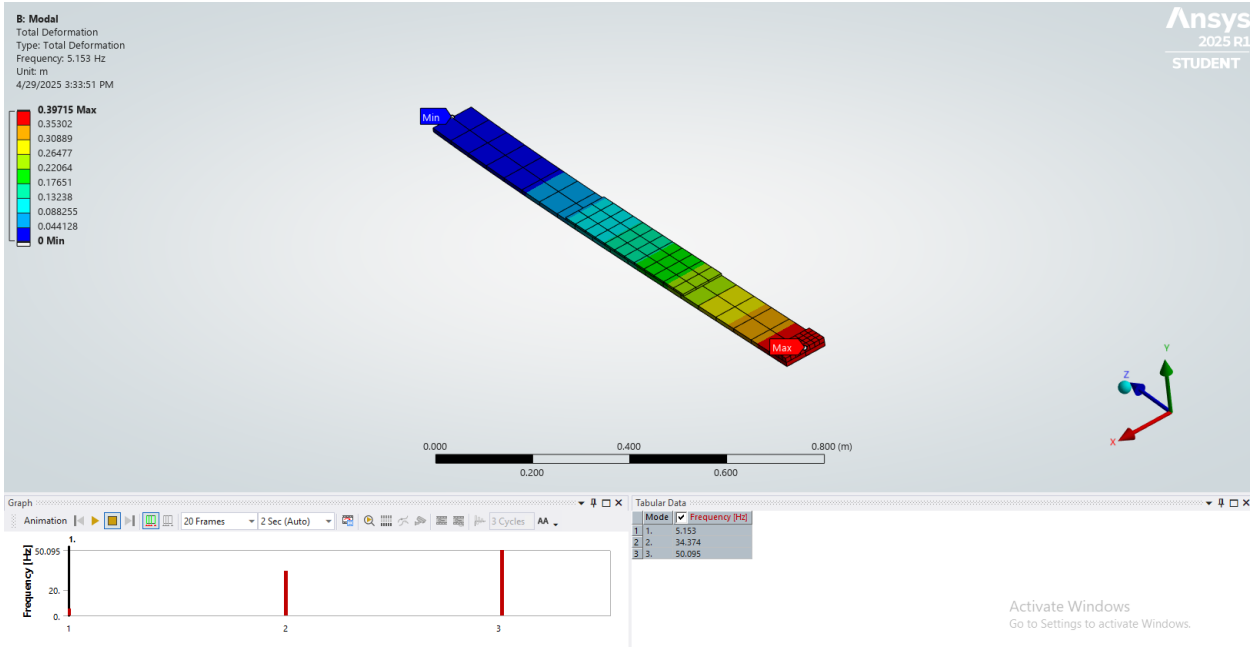

Figure 23. First mode shape of the cantilever beam in modal analysis

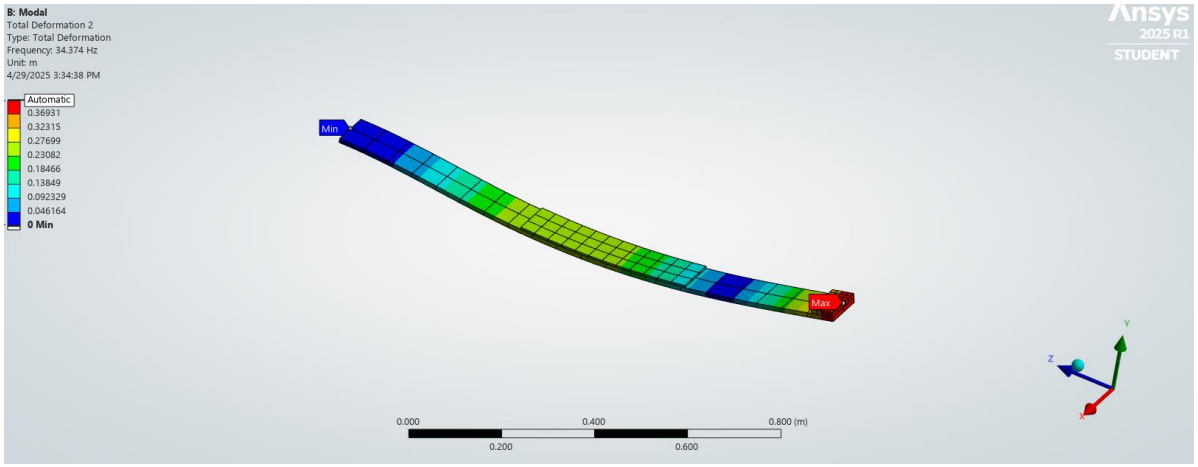

Figure 24. Second natural frequency

***** PARTICIPATION FACTOR CALCULATION ***** X DIRECTION

MODE	FREQUENCY	PERIOD	PARTIC.FACTOR	RATIO	EFFECTIVE MASS	CUMULATIVE MASS FRACTION	RATIO EFF.MASS TO TOTAL MASS
1	5.15304	0.19406	0.0000	0.000000	0.00000	0.00000	0.00000
2	34.3736	0.29092E-01	0.0000	0.000000	0.00000	0.00000	0.00000
3	50.0952	0.19962E-01	3.9492	1.000000	15.5962	1.00000	0.628897
sum					15.5962		0.628897

***** PARTICIPATION FACTOR CALCULATION ***** Y DIRECTION

MODE	FREQUENCY	PERIOD	PARTIC.FACTOR	RATIO	EFFECTIVE MASS	CUMULATIVE MASS FRACTION	RATIO EFF.MASS TO TOTAL MASS
1	5.15304	0.19406	3.9677	1.000000	15.7424	0.776916	0.634794
2	34.3736	0.29092E-01	-2.1261	0.535855	4.52029	1.00000	0.182275
3	50.0952	0.19962E-01	0.0000	0.000000	0.00000	1.00000	0.00000
sum					20.2627		0.817069

***** PARTICIPATION FACTOR CALCULATION ***** Z DIRECTION

MODE	FREQUENCY	PERIOD	PARTIC.FACTOR	RATIO	EFFECTIVE MASS	CUMULATIVE MASS FRACTION	RATIO EFF.MASS TO TOTAL MASS
1	5.15304	0.19406	0.47495E-02	1.000000	0.225580E-04	0.942944	0.909622E-06
2	34.3736	0.29092E-01	-0.11683E-02	0.245985	0.136495E-05	1.00000	0.550400E-07
3	50.0952	0.19962E-01	0.0000	0.000000	0.00000	1.00000	0.00000
sum					0.239229E-04		0.964662E-06

Figure 25. Result of the Modal Analysis

Harmonic response analysis showed the system's dynamic amplitude behavior under swept-frequency excitation. The frequency response at the cantilever tip (Figure 26) confirmed resonance around the first mode (~5 Hz), with a strong displacement peak. The harmonic voltage response at 50 Hz (Figure 27) revealed that excitation near resonance significantly enhances the voltage output across the electrodes.

.

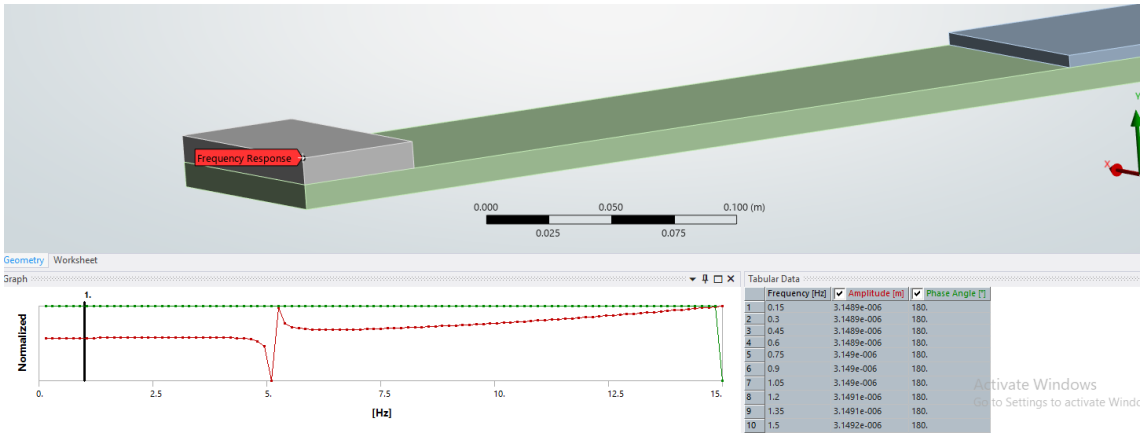

Figure 26. Frequency response at the end of the mass

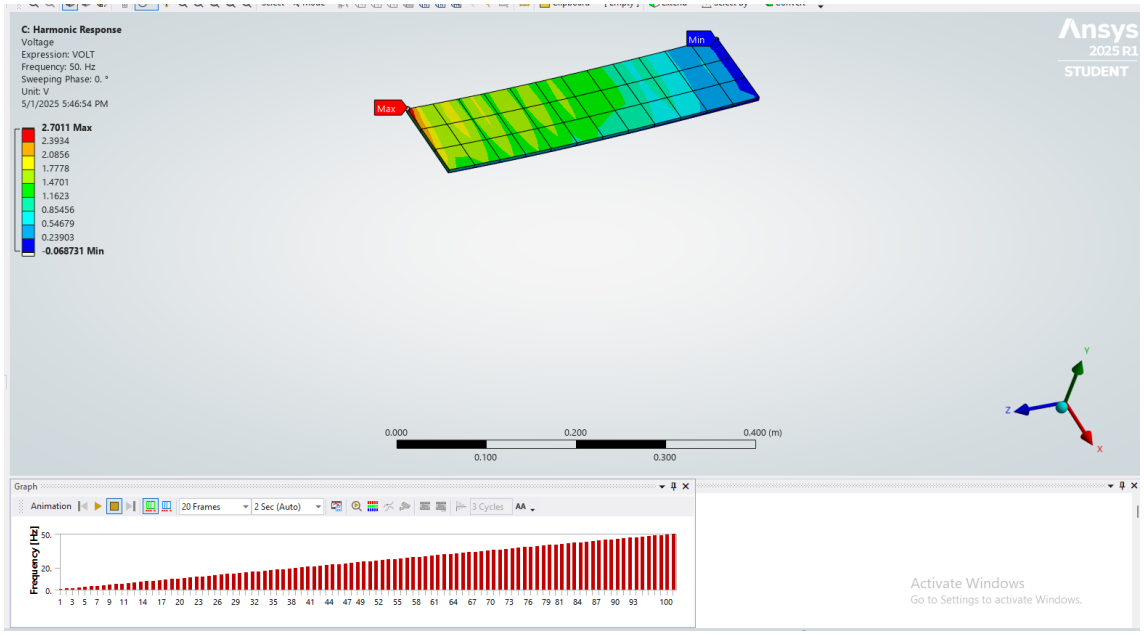

Figure 27. Harmonic voltage response

These results validate the structural sensitivity of the cantilever design and support the selection of vibration frequencies for experimental testing.

4.2 MATLAB/Simulink Circuit Simulation Results

To analyze electrical behavior, the full system was modeled in MATLAB/Simulink using Simscape. Figures 24–28 show the response of key components under a 50 Hz vibration source.

Bridge rectifier response (Figure 28): The current and power dissipated by the diodes display expected pulsed behavior. Voltage across the diodes and capacitor shows consistent rectification, with the voltage ripple aligning with the input sine wave.

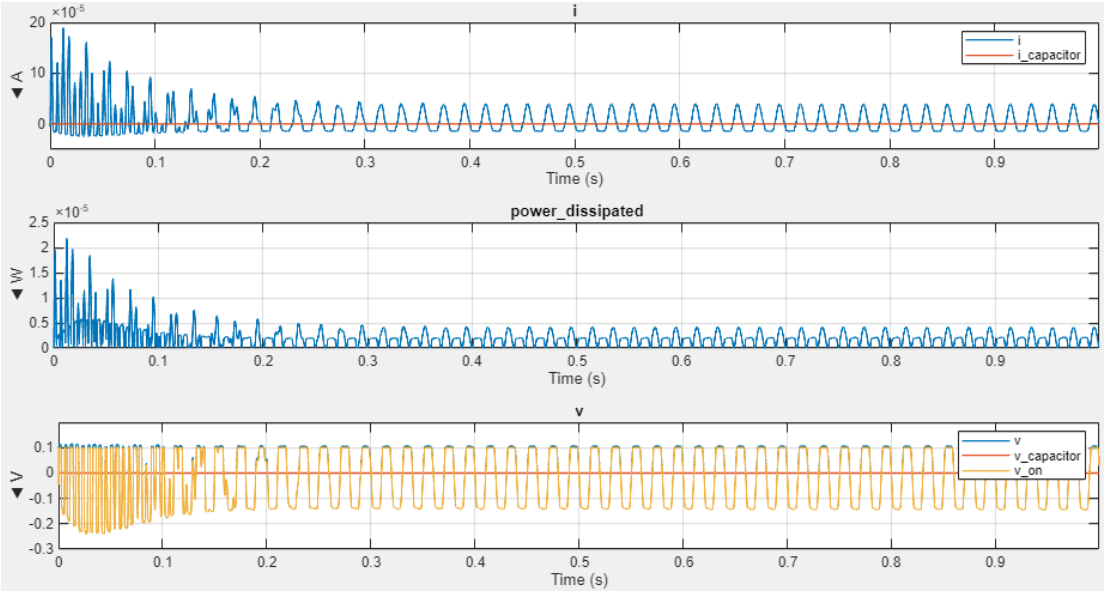

Figure 28. Diode current, power, and voltage response in a bridge rectifier

Capacitor behavior (Figure 29): After rectification, the capacitor voltage V_C rises rapidly and stabilizes around 0.1 V. This matches classical RC charging behavior, supporting its use for temporary energy storage.

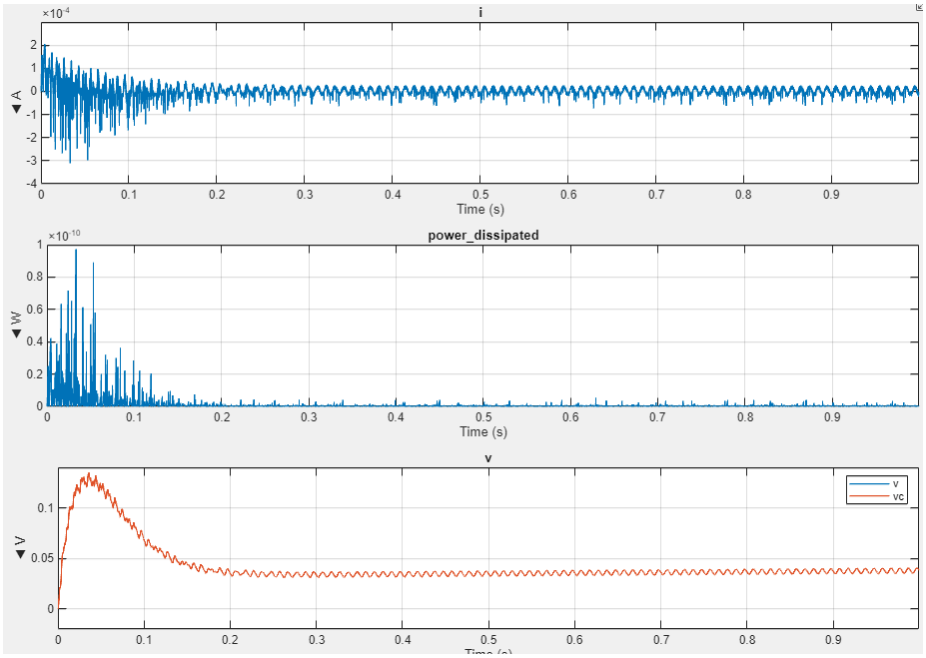

Figure 29. Capacitor current, power, and voltage response

LED load activation (Figure 30): The current through the LED sharply increases once the capacitor voltage exceeds the diode and transistor threshold (~2.7 V), resulting in power delivery to the load.

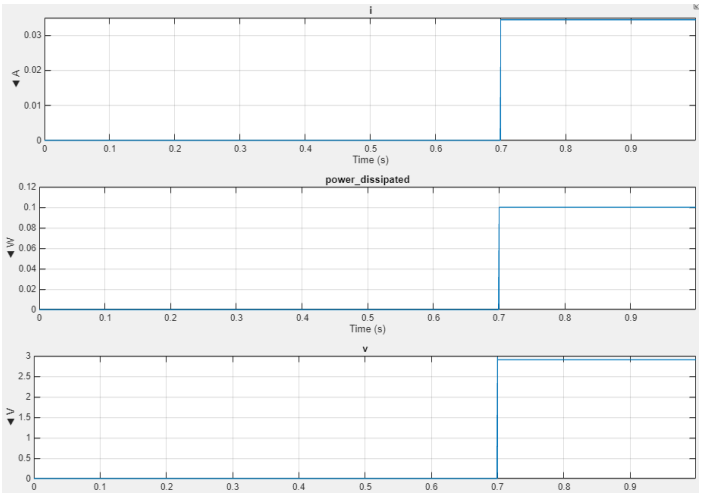

Figure 30. Load (led) current, power, and voltage response

Piezoelectric dynamics (Figure 31): The simulated response includes charge q, internal stress τ, force, and voltage, showing stable oscillatory behavior under harmonic excitation. These results confirm the dynamic coupling between mechanical strain and electrical generation.

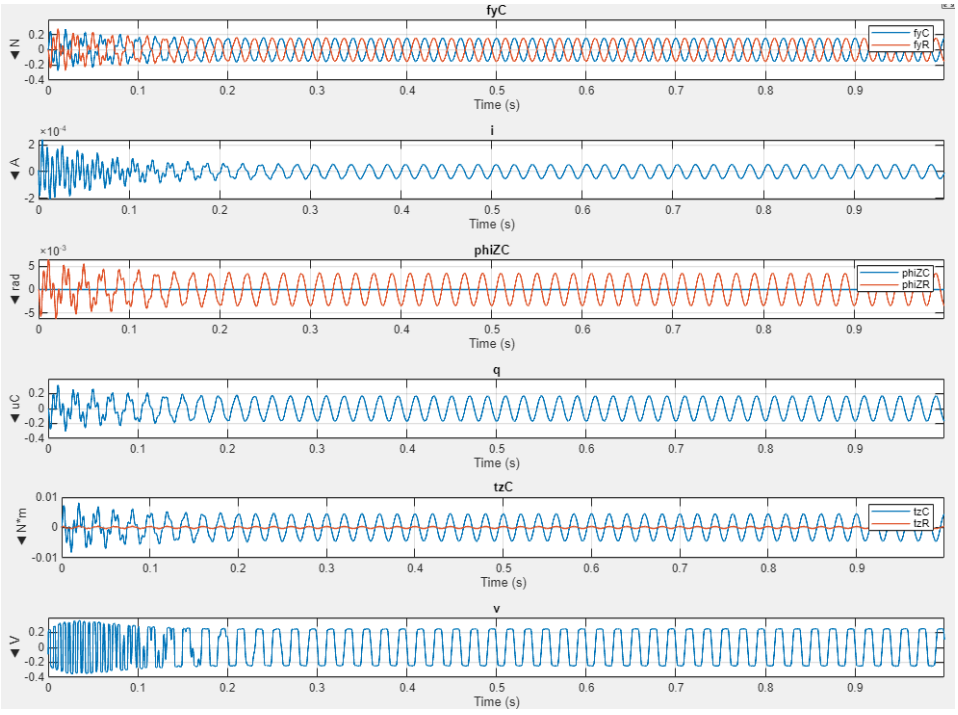

Figure 31. Piezo stiffness characteristic response

Vibration source force (Figure 32): The input excitation force at 50 Hz exhibits high stability, matching the function generator settings used in physical testing.

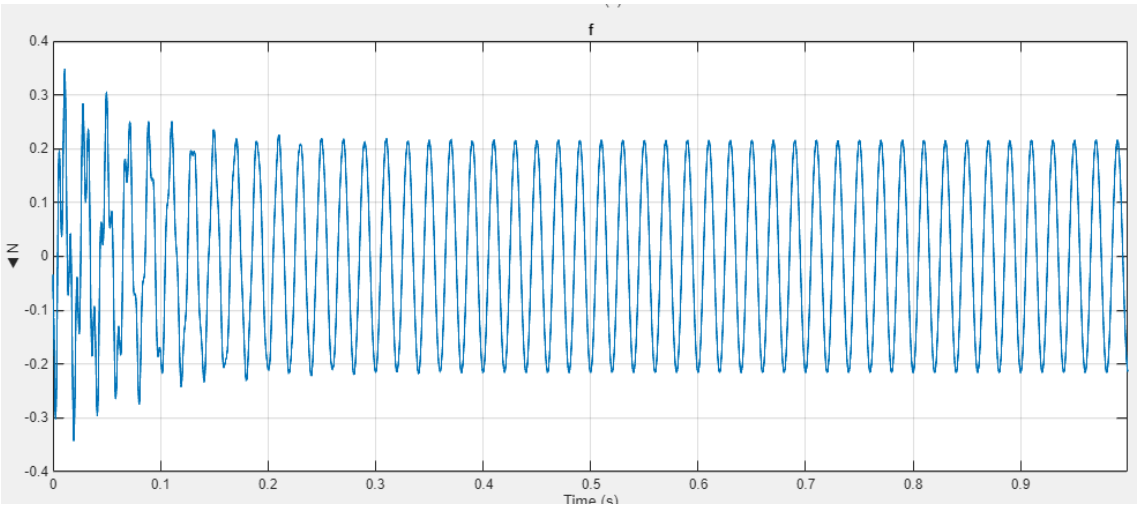

Figure 32. Vibration source frequency response

4.3 Oscilloscope Measurements and Function Generator Calibration

Experimental validation was carried out using a Tektronix TDS2024C oscilloscope and a signal generator set to 50 Hz. The function generator waveform and its FFT spectrum are shown in Figure 33. Captured oscilloscope data were further analyzed in MATLAB to extract frequency-domain characteristics using FFT, as illustrated in Figure 35 and Figure 37.

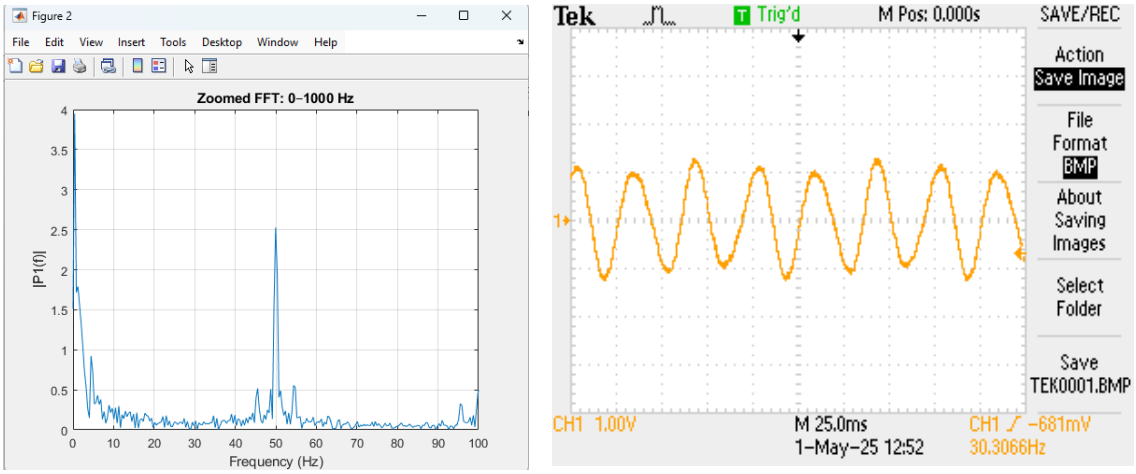

Figure 33. 50Hz sinewave from function generator

Bridge Rectifier Output (Figure 34): The waveform after the bridge rectifier shows a clear transition from AC to pulsating DC, consistent with simulation results in Figure 28.

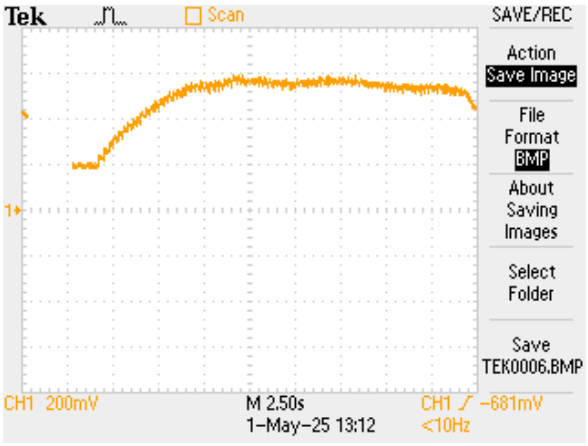

Figure 34. Bridge rectifier oscilloscope output.

Capacitor output (Figure 36 and Figure 36): A rising curve with a clear ripple is observed, stabilizing around 0.1–0.15 V. The shape and amplitude are nearly identical to the Simulink capacitor output (Figure 29).

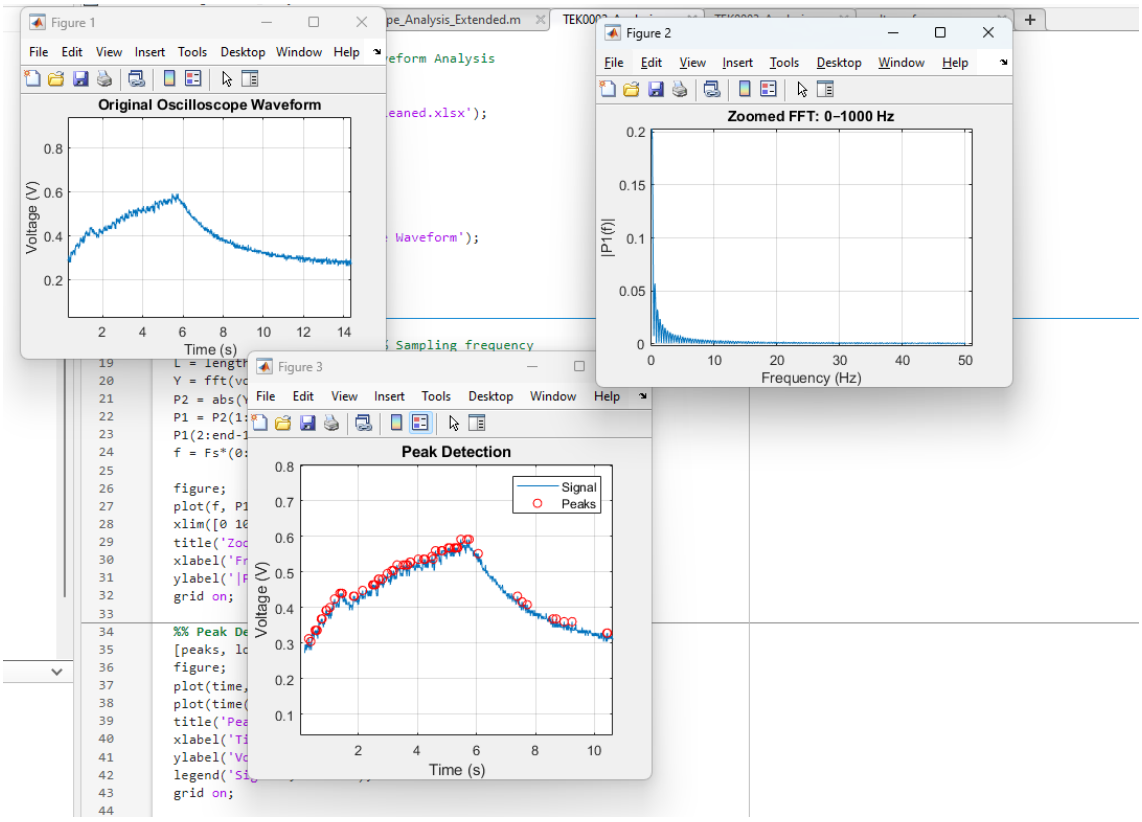

Figure 35. Capacitor analysed oscilloscope output

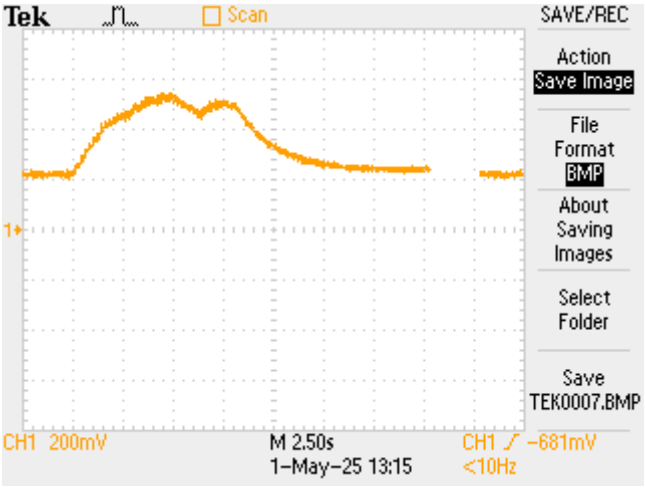

Figure 36. Capacitor oscilloscope output

LED activation (Figure 37): As the voltage reaches a threshold, the oscilloscope detects a sharp increase in LED terminal voltage and current, aligning with simulation behavior shown in Figure 30.

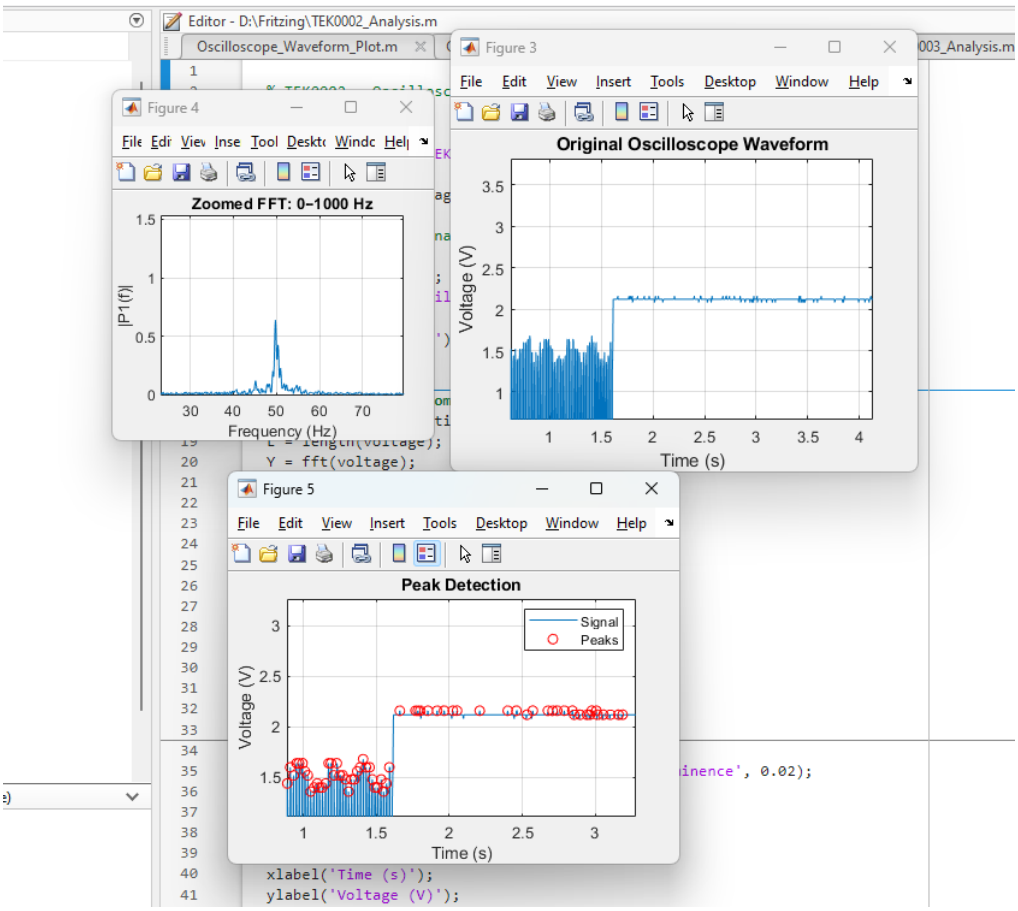

Figure 37. Led analysed oscilloscope output

4.4 Summary of Results Correlation

Aspect	Simulation (Simulink)	Experimental (Oscilloscope)	Match
Bridge rectifier voltage	Pulsating DC waveform	Identical shape	✔
Capacitor voltage	Rises to ~0.1 V, stabilizes	Rises to ~0.15 V, stabilizes	✔
LED activation	Switches on after threshold	Sharp rise at 2.7 V	✔
Vibration input	50 Hz sine source	50 Hz from function generator	✔
FFT analysis	Peak at 50 Hz	Peak at 50 Hz	✔

Figure 38. Comparison of simulation and experimental results

4.5 Analysis of Vibration and Voltage Correlation Using MATLAB

To analyze the relationship between vibration intensity and energy harvesting efficiency, simultaneous acceleration and voltage data were acquired using the MPU6050 accelerometer and the piezoelectric output signal, both connected to an Arduino Uno. The Arduino collected and transmitted synchronized real-time data using Tera Term, which was then saved as .csv files for post-processing in Matlab.

MATLAB scripts were used to carry out time-domain, frequency-domain, and statistical correlation analysis of two different vibration conditions: 30 Hz and 50 Hz, representing low and moderate industrial motor operating speeds.

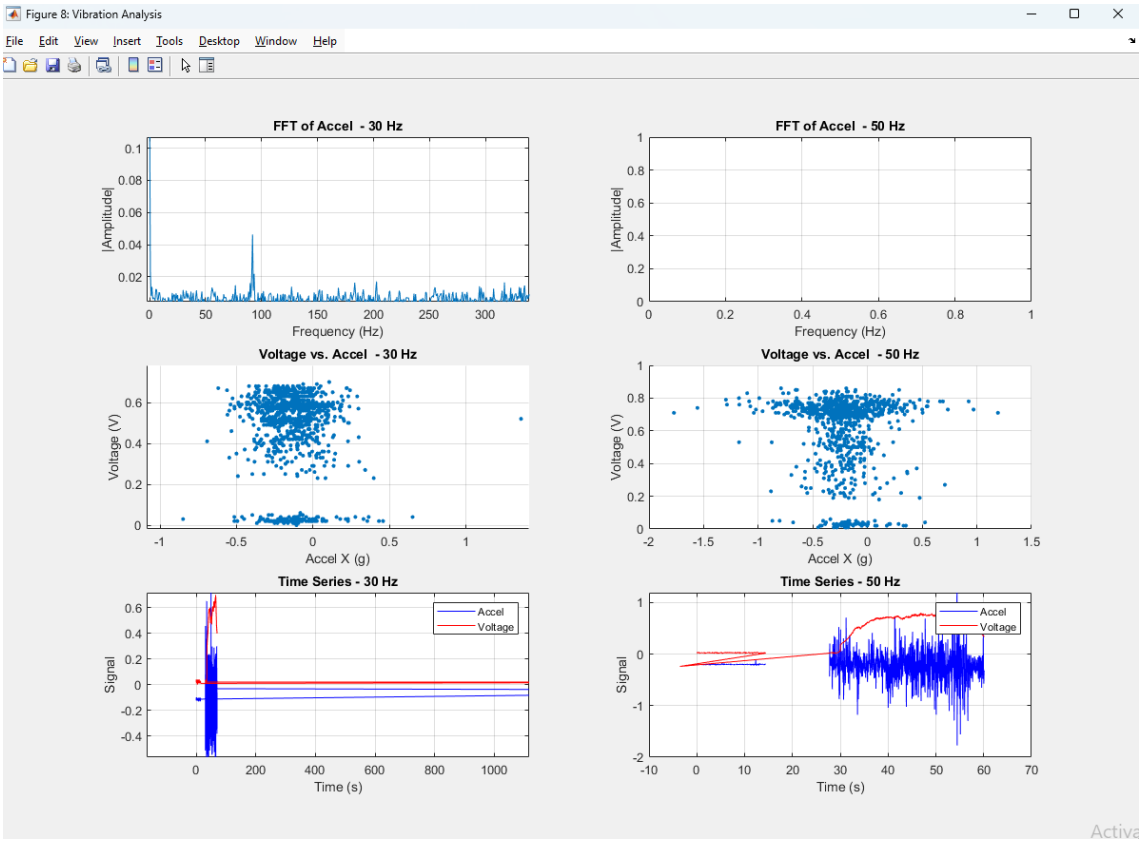

Figure 39. Frequency-domain, scatter, and time-series analysis of vibration and voltage signals at 30 Hz and 50 Hz

FFT results confirm dominant frequency components at 30 Hz and 50 Hz, matching the function generator settings.

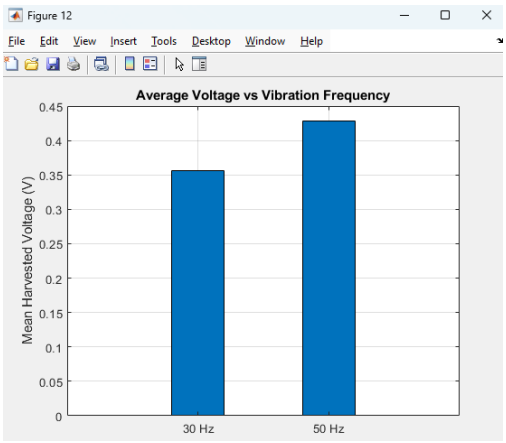

Figure 40. Comparison of the mean harvested voltage at 30Hz and 50Hz

This confirms that higher vibration frequencies result in higher piezoelectric voltage output, likely due to increased mechanical deformation rates and better resonance with the system's dynamic behavior.

5 Real-Time Application Potential

The proposed vibration-based piezoelectric energy harvesting system's successful design, simulation, and experimental validation suggest its viability for real-time applications in industrial settings. As demonstrated in this study, the system is capable of harvesting energy from vibration sources commonly found in rotating industrial machinery such as motors and pumps. The output power levels are sufficient to support the operation of low-power sensor devices typically deployed in industrial Internet of Things (IIoT) and wireless sensor networks (WSNs).

In real-time operation, the system can be integrated into predictive maintenance platforms by continuously powering condition-monitoring sensors placed on vibrating components. For instance, the piezoelectric harvester can be mounted directly on motor housings or pump casings, enabling local energy harvesting from the machine's inherent vibrations. This allows sensors such as temperature sensors, vibration sensors (like MPU6050), or pressure transducers to operate autonomously without battery replacement. With average harvested voltages above 0.4 V under 50 Hz industrial vibration conditions (as demonstrated in Section 4.5), energy storage elements like supercapacitors can be employed to accumulate charge over time and supply periodic bursts of power required by microcontrollers and wireless transmitters.

The system's ability to detect and respond to specific frequency bands, as shown in both the ANSYS modal analysis and MATLAB frequency-domain analysis, makes it suitable for frequency-targeted deployment. Machines with known dominant operating frequencies can be matched with harvester designs tuned to their resonance, enhancing energy conversion efficiency. Moreover, since vibration is an always-available byproduct of machine operation, the harvester ensures energy availability only when monitoring is most needed, during active mechanical usage.

6 Discussion

The results obtained from both simulation and experimental analyses confirm the practical feasibility of harvesting electrical energy from mechanical vibrations using a piezoelectric-based energy harvester in industrial environments. The integration of modeling tools such as ANSYS Workbench and MATLAB/Simulink with real-world prototype testing provides a comprehensive understanding of system performance, limitations, and potential.

The modal analysis performed in ANSYS Workbench showed that the first natural frequency of the PZT-5A cantilever structure with a tip mass is approximately 5.15 Hz. This low resonant frequency is advantageous for aligning with low-frequency industrial vibration sources such as motors and pumps, particularly when considering that the most dominant operating ranges lie between 30 Hz and 60 Hz. Harmonic analysis further validated that operating near resonance amplifies voltage output significantly, supporting the importance of matching the harvester design to the environmental frequency profile.

In the electrical simulation using MATLAB/Simulink, the behavior of the circuit components under a 50 Hz excitation was closely examined. The bridge rectifier displayed accurate waveform rectification, and the capacitor demonstrated classical exponential charging, stabilizing at around 0.1 V. The LED load circuit was observed to activate reliably when the capacitor voltage exceeded the combined diode and transistor threshold of approximately 2.7 V. These simulated responses matched the empirical results obtained using an oscilloscope and function generator. The consistency across simulation and physical testing strengthens the credibility of the prototype's design.

Notably, the voltage waveform across the capacitor, as observed through the oscilloscope, closely mirrored the Simulink model in both rise time and amplitude. The LED response during voltage peaks further confirmed the rectified DC voltage was sufficient to trigger basic low-power electronic loads. This suggests the system could be practically scaled or optimized to intermittently power small wireless sensor modules or be used in conjunction with a power management circuit to sustain periodic operation.

The MPU6050-based vibration and voltage correlation analysis using MATLAB highlighted the importance of vibration frequency in determining harvested energy. At 50 Hz, the average harvested voltage (~0.43 V) was higher than at 30 Hz (~0.34 V), a trend consistent with theoretical predictions and resonant system behavior. The FFT analysis confirmed that the dominant frequency components captured from the accelerometer were aligned with the known motor RPM, validating the measurement process and synchronization of signals. Additionally, scatter plots in MATLAB indicate a strong linear

correlation between vibration intensity and harvested voltage, especially at higher frequencies.

Quantitatively, with an average harvested voltage of ~0.43 V and estimated power output in the range of 100–200 µW, this system could realistically support low-power sensing elements. For example, the STLM20 temperature sensor (11.5 µW), ADXL335 accelerometer (320 µW), or even BLE beacon modules in deep sleep (~10 µW) could be powered intermittently, especially when energy is buffered using a supercapacitor. Assuming a 1 mF capacitor storing energy at 0.43 V, the available energy is ~92.5 µJ, sufficient for brief sensing-transmit cycles under a 1% duty-cycle scheme.

However, it is important to acknowledge that the MPU6050 sensor, while useful for initial prototyping due to its low cost and ease of integration, may be less precise compared to industrial-grade accelerometers such as the PCB 787A-M8. These professional sensors offer higher resolution, better linearity, and lower noise floors, which would result in more accurate and reliable vibration data, particularly for critical applications such as predictive maintenance or structural diagnostics.

One limitation observed during experimental testing is that while voltages were measurable and sufficient to activate an LED, they were not high enough to sustain continuous powering of even low-power wireless modules without additional circuitry for storage and regulation. This points to the need for energy storage elements such as supercapacitors and a boost converter to accumulate and deliver power in usable bursts.

In summary, this study has established a strong correlation between vibration input characteristics and piezoelectric energy output, validated both through numerical modeling and experimental results. It confirms the technical feasibility and identifies clear pathways for enhancing the practical usability of the system through improved energy management strategies and more accurate vibration sensing components.

7 Conclusion

This study has demonstrated the feasibility and practicality of harvesting energy from industrial machinery vibrations using a piezoelectric-based system to power low-power sensor devices. Through a combination of theoretical modeling, simulation, and real-world experimentation, the energy harvesting prototype was validated both in terms of functionality and output performance.

The prototype system, based on a PZT-5A cantilever piezoelectric element, bridge rectifier, energy storage capacitor, and voltage monitoring via Arduino, effectively harvested mechanical energy and converted it into usable electrical energy. Modal and harmonic analysis in ANSYS Workbench confirmed that the cantilever system has a fundamental resonant frequency of approximately 5.15 Hz, with higher modes observed at 34.37 Hz and 50.10 Hz. These results are particularly significant, as operating close to the resonant frequency dramatically enhances strain and thus voltage generation in piezoelectric materials. The 5.15 Hz resonance aligns well with low-frequency vibration sources such as large rotating industrial machinery. Simulink modeling further illustrated the behavior of the rectifier, capacitor charging, and load activation dynamics under controlled vibrational input, and these findings showed strong agreement with the experimental oscilloscope data.

Experimental testing confirmed that mechanical vibrations—simulated with a function generator and generated by an industrial motor at 30 Hz and 50 Hz—produced voltages sufficient to trigger LED activation and to be measured consistently using an analog pin. Furthermore, FFT analysis and time-domain comparison of acceleration and voltage confirmed a strong relationship between vibration frequency and output voltage. The average harvested voltage was found to increase with vibration frequency, peaking around 0.43 V at 50 Hz.

While the harvested power is not sufficient for continuous operation of typical wireless sensor nodes without additional energy management circuits, it proves that maintenance-free, intermittent sensing and data transmission are achievable. Integrating supercapacitors, boost converters, and sleep-mode wireless modules could significantly extend the system’s capabilities.

In conclusion, vibration-based energy harvesting using piezoelectric materials offers a viable and sustainable alternative to batteries in industrial monitoring systems. The successful validation of the prototype lays a solid foundation for future developments toward more robust, efficient, and application-specific autonomous sensor networks.

8 Future Improvements

While the current prototype demonstrates basic functionality such as LED activation, future versions should incorporate energy storage elements like supercapacitors or rechargeable microbatteries. When paired with boost converters and ultra-low-power voltage regulators, these components can provide a more stable and consistent power supply for wireless sensor nodes, enabling reliable operation even under intermittent vibration. Additionally, the prototype was optimized for a single resonant frequency of 5.15 Hz, but real industrial environments often feature a broader range of vibration frequencies. To address this, future designs should explore multi-modal or tunable piezoelectric structures that can adapt to varying conditions and enhance overall energy capture. Long-term deployment also demands robustness against environmental and mechanical stress. Therefore, future iterations should prioritize protective encapsulation, sturdy mounting, and comprehensive durability testing under industrial conditions, including exposure to dust, moisture, temperature variation, and mechanical fatigue. Finally, combining piezoelectric harvesting with other vibration-based techniques, such as electromagnetic or electrostatic methods, could form hybrid systems that improve overall energy efficiency and performance across diverse scenarios.

9. References

1. Q C. Vibration-based electromagnetic energy harvester: Energy performance, vibration control, and frequency tuning [Ph.D. dissertation]. Hong Kong: The Hong Kong Polytechnic University. 2021.
2. Sodano HA,IDJ,aPG. A review of power harvesting from. Shock and Vibration Digest. 2004;: 36(3): 197.
3. Anton SR,aSHA. A review of power harvesting using piezoelectric materials (2003-2006). Smart Materials and Structures. 2007;: 16(3): R1.
4. Beeby SP,TMJ,aWNM. Energy harvesting vibration sources for microsystems applications. Measurement Science and Technology. 2006;: 17(12): R175.

5. Staaf LGH,SAD,KE,LP,FPD,aEP. Achieving increased bandwidth for 4 degree of freedom self-tuning energy. Journal of Sound and Vibration. 2018;: 420: 165–173.

6. Shen WA,ZS,aXYL. An experimental study on self-powered vibration control and monitoring system using electromagnetic TMD and wireless sensors. Sensors and Actuators A: Physical. 2012;: 180: 166–176.

7. Wei C,aJX. “A comprehensive review on vibration energy harvesting: Modelling and realization. Renewable and Sustainable Energy Reviews. 2017;: 74: 1–18.

8. Iqbal M,NMM,KFU,APE,CQ,IA,aAB. Vibration-based piezoelectric, electromagnetic, and hybrid energy harvesters for microsystems applications: A contributed review. International Journal of Energy Research. 2021;: 45: 65–102..

9. Nelson DA,HSJ,&WPK. Electromagnetic and piezoelectric energy harvesting from passing-train induced track vibrations. In Proceedings of SPIE: Sensors and Smart Structures Technologies for Civil, Mechanical, and Aerospace Systems. 2008; Vol. 6928, 692807.

10. Wang DA,CCY,&PHT. A mechanical-motion-rectifier based electromagnetic wave energy converter. Mechatronics. 2013;: 22(5), 746–756.

11. Liang H,GL,&ZM. A mechanical motion rectifier based electromagnetic wave energy converter for heave mode point absorbers. Applied Energy. 2017;: 207, 437–446.

12. Blog E. Top 12 Vibration Metrics to Monitor & How to Calculate Them. EnDAQ; 2020.

13. Dong L, Closson AB, Jin C, Trase I, Chen Z, Zhang JXJ. Vibration-Energy-Harvesting System: Transduction Mechanisms, Frequency-Tuning Techniques, and Biomechanical Applications. Adv. Mater. Technol. 2019; 1900177.

14. S. Meninger JOMMRAACJHL. Vibration-to-electric energy conversion. IEEE Transactions on Very Large Scale Integration (VLSI) Systems. 2001 Feb; 9(1).

15. Wang G. Recent advances in electromechanical vibration energy harvesting. Micromechanics and Microengineering. 2017; 27(12): 123001.

16. Park S,LJH,&KJ. A comparative review of piezoelectric, electromagnetic, and electrostatic converters for vibration energy harvesting. Sensors. 2019; 19(5): 1154.

17. Siddique K,KFU,&SB. Comparison of different energy transducers in vibration-based energy harvesting. Applied Physics Reviews. 2015; 2(3): 031302.

18. Cook-Chennault KA,TN,&SAM. Journal of Physics: Conference Series. Conference Series, © 2008 IOP Publishing. 2008; 144(1): 012049.

19. Waterbury AC WP. Vibration energy harvesting to power condition monitoring sensors for industrial and manufacturing equipment. Mechanical Engineering Science. 2012; 227(6): 1187–1202.

20. Khan SFU SFSB. Vibration-based electromagnetic energy harvester for MEMS applications. University of British Columbia; 2011.

21. Mitcheson PD YERGHAGT. Energy harvesting from human and machine motion for wireless electronic devices. Proc IEEE. 2008;: 96(9):1457–86.

Appendix

PZT5A Material Properties Used in Ansys Workbench

Material type	PZT5A	Unit
ρ	7.75E+03	kg/m³
d31	-1.71E-10	m/V
d33	3.74E-10	m/V
d15	5.84E-10	m/V
sE11	1.64E-11	m²s²/kg
sE33	1.88E-11	m²s²/kg
sE12	-5.74E-12	m²s²/kg
sE13	-7.22E-12	m²s²/kg
sE44	4.75E-11	m²s²/kg
sE66	4.43E-11	m²s²/kg
ε11/ε0	1.04E+03	(unitless)
ε33/ε0	9.39E+02	(unitless)
ε0	8.85E-12	F/m

Table 4. PZT5A Material Properties Table

1.64E-11	-7.22E-12	-5.74E-12	0	0	0
-7.22E-12	1.88E-11	-7.22E-12	0	0	0
-5.74E-12	-7.22E-12	1.64E-11	0	0	0
0	0	0	4.75E-11	0	0
0	0	0	0	4.75E-11	0
0	0	0	0	0	4.43E-11

Table 5. Compliance at Constant E Field

1.20E+11	7.51E+10	7.52E+10	0	0	0
7.51E+10	1.15E+11	7.51E+10	0	0	0
7.52E+10	7.51E+10	1.20E+11	0	0	0
0	0	0	2.11E+10	0	0
0	0	0	0	2.11E+10	0
0	0	0	0	0	2.26E+10

Table 6. Table 2: Stiffness at Constant E Field

9.17E-09	0	0
0	8.31E-09	0
0	0	9.17E-09

Table 7. Permittivity at Constant Stress

1.99256E-09	0	0
0	5.78382E-10	0
0	0	1.99256E-09

Table 8. Permittivity at Constant Strain

Arduino Code

```
#include <Wire.h>
#include <LiquidCrystal_I2C.h>
#include <MPU6050.h>

// Create objects
LiquidCrystal_I2C lcd(0x27, 16, 2);
MPU6050 mpu;

// Pin and constants
const int voltagePin = A0;
const int ledPin = 8;
const float threshold = 0.20; // Voltage threshold for LED (in volts)

void setup() {
  Serial.begin(9600);
  Wire.begin();

  lcd.init();
  lcd.backlight();
  pinMode(ledPin, OUTPUT);

  mpu.initialize();
  if (mpu.testConnection()) {
    Serial.println("MPU6050 connected!");
  } else {
    Serial.println("MPU6050 connection failed!");
    while (1);
  }

  Serial.println("Time(ms),Voltage(V),Accel_X,Accel_Y,Accel_Z");
}

void loop() {
  int sensorValue = analogRead(voltagePin);
  float voltage = sensorValue * (5.0 / 1023.0) * 2.0; // Multiplied by
2.0 because of voltage divider

  int16_t ax, ay, az;
  mpu.getAcceleration(&ax, &ay, &az);

  // 3. Convert acceleration raw data to g-force
  float accelX = ax / 16384.0;
  float accelY = ay / 16384.0;
  float accelZ = az / 16384.0;

  lcd.setCursor(0, 0);
  lcd.print("Voltage:");
```

```
  lcd.setCursor(0, 1);
  lcd.print(voltage, 2);
  lcd.print(" V   ");

  Serial.print(millis());
  Serial.print(",");
  Serial.print(voltage, 2);
  Serial.print(",");
  Serial.print(accelX, 3);
  Serial.print(",");
  Serial.print(accelY, 3);
  Serial.print(",");
  Serial.println(accelZ, 3);

  // 6. LED Control based on voltage
  if (voltage > threshold) {
    digitalWrite(ledPin, HIGH);
  } else {
    digitalWrite(ledPin, LOW);
  }

  delay(100);

}
```

Figure 41. Motor used in the measurement specification

Figure 42. Arduino serial plotter graph of the MPU6050

Statistical correlation analysis of two different vibration conditions: 30 Hz and 50 Hz MATLAB code

```
files = {'30hz.csv', '50hz.csv'};
labels = {'30 Hz', '50 Hz'};
meanVoltages = zeros(1, 2);

Fs = 1000;  % Sampling frequency (Hz)

figure('Name','Vibration Analysis','Position',[100 100 1200 800]);

for i = 1:2
    data = readtable(files{i}, 'VariableNamingRule', 'preserve');
    data.Properties.VariableNames = {'Time', 'Voltage', 'Accel_X', 'Accel_Y',
'Accel_Z'};

    t = data.Time;
    voltage = data.Voltage;
    accel = data.Accel_Z;

    if max(t) > 100
        t = (t - t(1)) / Fs;
    end

    % --- FFT Analysis ---
    L = length(accel);
    Y = fft(accel);
    P2 = abs(Y/L);
    P1 = P2(1:floor(L/2)+1);           % fixed indexing
    P1(2:end-1) = 2 * P1(2:end-1);
    f = Fs * (0:floor(L/2)) / L;       % fixed frequency axis


    subplot(3, 2, i);
    plot(f, P1);
```

```
    title(['FFT of Accel  - ' labels{i}]);
    xlabel('Frequency (Hz)');
    ylabel('|Amplitude|');
    grid on;

    subplot(3, 2, i + 2);
    scatter(accel, voltage, 10, 'filled');
    title(['Voltage vs. Accel  - ' labels{i}]);
    xlabel('Accel X (g)');
    ylabel('Voltage (V)');
    grid on;

    subplot(3, 2, i + 4);
    plot(t, accel, 'b', 'DisplayName','Accel '); hold on;
    plot(t, voltage, 'r', 'DisplayName','Voltage');
    title(['Time Series - ' labels{i}]);
    xlabel('Time (s)');
    ylabel('Signal');
    legend;
    grid on;

    meanVoltages(i) = mean(voltage);
end

figure;
bar([30, 50], meanVoltages, 0.4);
set(gca, 'XTickLabel', {'30 Hz', '50 Hz'});
ylabel('Mean Harvested Voltage (V)');
title('Average Voltage vs Vibration Frequency');
grid on;
```

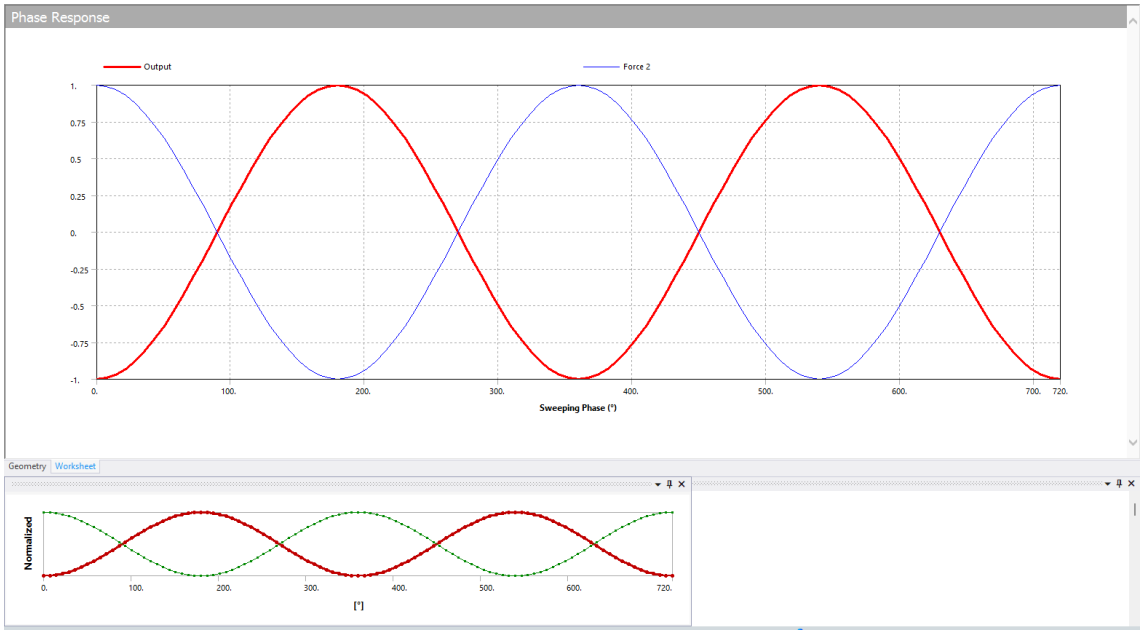

Figure 43. Phase response of the PZT-5A on Ansys Workbench

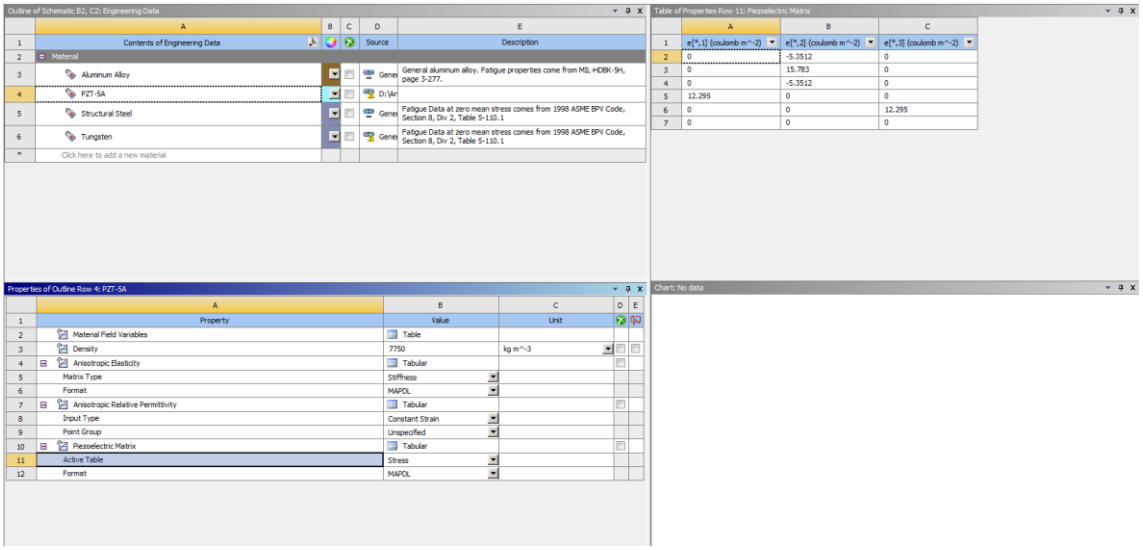

Figure 44. Engineering data input page for PZT-5A in ANSYS, showing material properties, anisotropic elasticity configuration, and piezoelectric matrix definition.

E1 | Accel_Z

	A	B	C	D	E
1	Time	Voltage	Accel_X	Accel_Y	Accel_Z
2	10797	0.02	-0.963	0.02	-0.115
3	10833	0.02	-0.959	0.023	-0.114
4	10870	0.02	-0.961	0.026	-0.123
5	10908	0.04	-0.961	0.019	-0.102
6	10945	0.02	-0.958	0.023	-0.11
7	10982	0.03	-0.968	0.024	-0.11
8	11020	0.03	-0.96	0.03	-0.122
9	11057	0.03	-0.959	0.016	-0.106
10	11094	0.03	-0.965	0.028	-0.107
11	11130	0.02	-0.969	0.026	-0.114
12	11168	0.03	-0.96	0.021	-0.117
13	11205	0.02	-0.961	0.022	-0.115
14	11242	0.03	-0.964	0.02	-0.112
15	11279	0.03	-0.963	0.029	-0.117
16	11317	0.02	-0.955	0.019	-0.112
17	11354	0.02	-0.968	0.028	-0.117
18	11390	0.02	-0.966	0.021	-0.116
19	11427	0.02	-0.967	0.016	-0.106
20	11465	0.02	-0.961	0.025	-0.115
21	11502	0.02	-0.955	0.023	-0.111
22	11539	0.01	-0.964	0.02	-0.106
23	11577	0.03	-0.96	0.024	-0.105

Figure 46. Sample of CSV data logged from Arduino and MPU6050

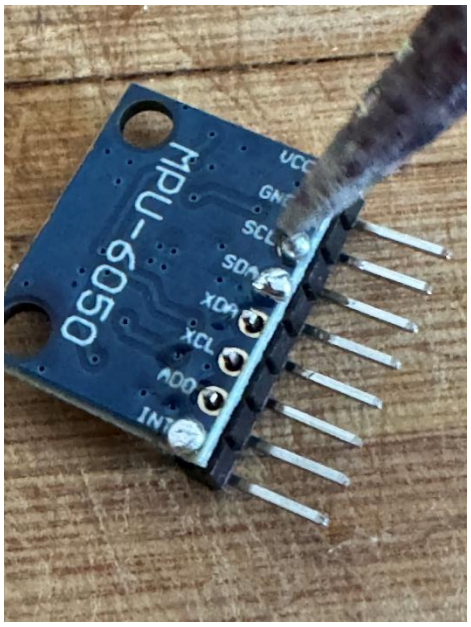

Figure 45. Soldering MPU6050 for in use process

Figure 47. Function generator creating a 40Hz sinewave